Università degli Studi di Padova

Dipartimento di Ingegneria Industriale

Corso di Laurea in Ingegneria Aerospaziale

Tesi di Laurea Magistrale

Analysis of the effect of different coatings on ejection forces in micro injection moulding

Relatore: Professor Giovanni Lucchetta
Correlatori: Dottor Marco Sorgato
Ingegner Davide Masato

Laureanda: Anna Pegoraro

ANNO ACCADEMICO 2016 – 2017

Typeset with LaTeX and gsm-l author class of $\mathcal{AMS}$ (American Mathematical Society).
Text and math typefaces are Kp-Fonts by Christophe Caignaert.

Velle est posse.

Alla mia mamma,
che mi ha insegnato tenacia e perseveranza.

Contents

List of Figures

List of Tables

List of Plots

Acronyms

COC: Cyclic Olefin Copolymer
CrTiNbN: Chromium Titanium Niobium Nidride
CVD: Chemical Vapor Deposition
DLC: Diamond Like Carbon
µEDM: micro Electrical Discharge Machining
PA: Polyamide
PACVD: Plasma Assisted Chemical Vapor Deposition
PC: Policarbonate
PET: Polyethylene terephthalate
PLD: Pulsed Laser Deposition
PMMA: Poly(methyl methacrylate)
POM: Polyoxymethylene
PP: Polypropylene
PS: Polystirene
PVD: Physical Vapor Deposition
SEM: Scanning Electron Microscope
µWEDG: micro Wire Electrical Discharge Grinding

Abstract

The purpose of this study was to investigate the effects of different mould coatings on ejection force in micro injection moulding, for a selection of thermoplastic polymers. Two semi-crystalline and two amorphous polymers were sorted. According to their potential affinity with the selected injected polymers, three different coatings were chosen: two types of Diamond Like Carbon (DLC) and a Chromium Titanium Niobium Nidride (CrTiNbN) coating. The mould cavity was designed to present interchangeable cores, this parts were manufactured by micro milling, than coated. In order to isolate the effect of polymer adhesion on the demoulding force, they were finally characterized in topography and geometry. Adhesion work was also correlated to the various combinations of injected polymers and surface coatings. Evaluating the interface contact angle between polymers and coated surfaces at the melt temperature, the wettability analysis was performed. In accordance with results of this work, the optimal mould coating should be selected, in order to minimize the ejection force for a certain polymer, considering its wettability properties.

Acknowledgements

A sincere and special thanks goes to Tommaso,
who with his essential help, support, patience and love made this work possible.

Anna Pegoraro

Padova, April 2017

Preface

All industrial fields, from automotive to biomedical, from aerospace to information technology, are developing systems that need light and thin components. Many technologies at the state of art are useful to manufacture micro devices, but micro injection moulding process is the most promising in terms of wide scale production and high precision products.

In injection moulding is increasing the demand regarding geometrical complexity and dimensional accuracy. Several technological issues are posed in particular in microfluidic devices, that are used in large variety of applications in healthcare sector (figure 1).

Principal aim of micro injection moulding development is manufacture of relative economical parts that can be produced respecting severe dimensional requirements in an almost automatic way. Injection moulding process is the most quick process among other manufacturing technologies, therefore it is a interesting research field in order to produce large quantities of good quality component in short time.

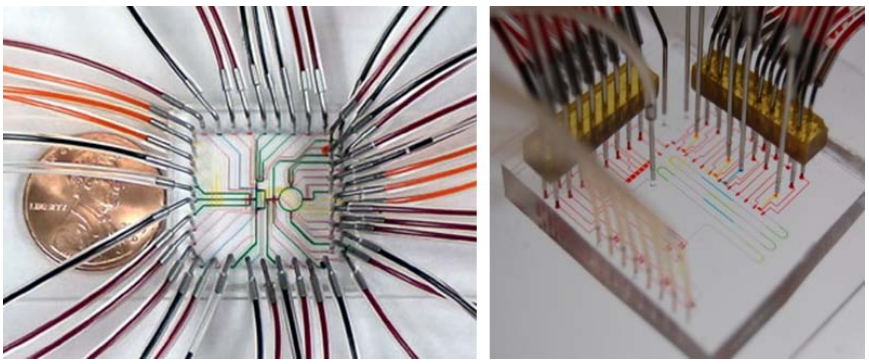

Figure 1. Microfluidic device manufactured by injection moulding.

Figure 2. Examples of micro devices produced by injection moulding.

Injection moulding technology allows usage of a wide range of mouldable polymer, making de facto every required device possible.

The only limitation to micro injection moulding process is given by geometry; because of the nature of the process itself, moulds cannot present undercuts or features with too elevated aspect ratio, otherwise the piece would not be extracted from the mould or polymer would cool down to early without completely fill mould cavity.

Micro parts are characterized by a larger surface in comparison with volume, thus cooling rate is higher: rapid cooling induces high shrinkage of polymer on mould walls and that is the major disadvantage of injection moulding technology, which has to be reduced.

Friction during ejection phase generates stresses in the moulded part that could lead to deformations or damages. To guarantee an high quality process thermal, chemical and tribological condition at polymer-mould interface have to be understood.

Ejection system of this technology consists in application of local forces through ejection rods in specific points of the part. Because of reduced dimensions of parts and small number of possible ejectors, local forces could be so high that distortions or fractures may occur. To obtain parts with required quality and tolerance ejection forces have to be reduced.

In order to reduce stresses at the interface between mould and part during ejection phase, many strategies can be adopted. In particular, from literature mould surface coatings seam to be a solution that permits to successfully improve tribological conditions at interface reducing ejection stresses. This work will investigate ejection forces at variation of mould coatings.

A surface coating can modify chemistry of interface between polymer and mould surface; polymers wettability properties could affect the filling and demoulding phases. Recent studies suggest that interfacial tension, which is the stress required to separate the viscous fluid from solid mould surface, could be used to

predict demoulding resistance (that is inversely proportional to friction). Hence, two materials with high interfacial tension are easy to separate. For this purpose wettability has to be evaluated considering the contact angle between plain surface and a drop of melted polymer.

Aim of the study. In this study, behaviour of four different materials during ejection phase from one uncoated and three coated moulds was evaluated. Rheological properties of polymers and tribological conditions at interface were considered, in order to refer results to the only interaction between polymer and coating material.

Outline. A general introduction to micro parts and micro injection moulding process is present in chapter 1; chapter 2 is a literature review of demoulding process and parameters that affect it.

Second part includes the experimental setup description: in chapter 3 materials and their properties are considered; chapter 4 resumes steps needed to mould production and chapter 5 is a particular presentation of injection moulding machine used.

Third part report experimental analyses carried: chapter 6 talks about surface characterization operations; chapter 7 presents results of wettability tests and chapter 8 defines the final evaluation of demoulding force.

In the end, chapter 9 summarizes researched work to conclude this study.

Part 1

Literature review

Chapter 1

Micro parts

There are several fields such as biomedical, automotive, telecommunication, information technology and aerospace, where micro devices are required.

Main reason why micro parts are developed is the necessity of a downsize product in order to have a lighter and smaller piece (particularly in aerospace industry) or a multifunction device that consumes less energy (for example micro chips in information technology). The research in micro technologies allows the realisation of new products and permits the development of high precision processes.

The definition of micro component depends on the used production technology and its characteristics. Since this study is based on micro injection moulding process, a part product by this technology can be defined in the following way according to [3]:

(1) mass of the component is few milligrams;

(2) tolerances of part dimensions belong to micro metric range;

(3) some features are estimated in the order of micro meters, or the wall thickness is minor than 100 µm.

In order to produce micro parts different materials can be used: polymers, glass or metals; replication is one of the most important capabilities that must be considered in the choice of right material for part production. In this study only polymeric materials were used.

Polymers can be divided in two big categories: thermoplastic and thermosetting.

Thermoplastic polymers: soften when temperature increases and harden when cooled. The process is reversible and repeatable with temperature variations. Material may degrade if temperature exceeds the level at which chemical bonds between monomers broke.

Thermosetting polymers: harden with rising temperature and do not soften any more if temperature increases again. The process is irreversible.

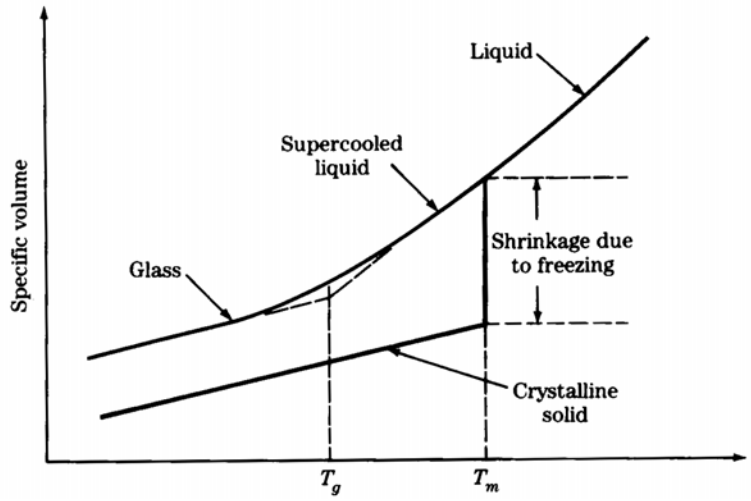

Figure 3. Relation between specific volume and temperature for polymeric materials.

In figure 3 is reported the schematic behaviour of polymer specific volume in relation with temperature variation. Two temperatures are to be considered in this analysis.

(1) T_g is the glass transition temperature around which a gradual transformation from a liquid to more viscous fluid happens. The inverse transformation occurs when the temperature increases.

(2) T_m is the melting temperature, i.e. the point beyond which the solid thermoplastic polymer becomes a viscous liquid.

Both T_g and T_m are important material characteristics useful to describe replication mechanisms.

The same figure shows how the material specific volume decreases with lower temperatures: this phenomenon is called shrinkage. During cooling different shrinkages between polymer and mould develop and stresses are generated in demoulding phase. Considering this effect the mould cavity should be designed with larger dimensions in comparison with the required size of the part.

Both injection moulding processes (micro and macro) require the polymers to meet severe operation conditions in terms of high temperature and pressure and in general all standard thermoplastic materials used for injection moulding are suitable also for micro process. The choice of the right polymer to mould depends on the physical properties the finished part need to present. Aspects linked to consequent device application, which are to be considered, belong to mechanical, thermal and chemical fields. Moreover electrical characteristics, optical properties or biocompatibility are to be investigated. In case of micro applications costs are less considered because of the small component sizes and the low material quantity required.

However polymers requirements are also to be researched in manufacturability of micro components. In fact different polymers influence the moulding efficiency with flowability, heat transfer ability and cooling shrinkage. In particular a polymer for micro injection moulding should present low viscosity to efficiently fill micro cavities: therefore most of micro injection moulding materials are low viscosity formulations of standard polymers.

1. Development of micro technologies

At the actual state of art micro parts have been successfully developed as prototypes in research laboratories, but costs are still too high for mass productions. In order to obtain cost effective manufacturing technologies, high production rate and accuracy should demonstrate high.

Micro moulding process permits to transfer precise micro structures designed on metallic moulds to moulded polymeric components. This process includes several technology among which there are injection moulding, reaction injection moulding, hot embossing, injection compression moulding and thermoforming [3] and [26].

Micro injection moulding: is the most promising process in order to have an economic mass production. Following steps describe a general injection moulding process: mould cavity is closed, evacuated and heated at a temperature major than polymer glass transition temperature; melted material is pushed and pressed into the cavity then the mould is cooled down again below glass transition temperature. In this way the solidified part can be demoulded.

Reaction injection moulding: is similar to injection moulding, but it uses two component as injection material: this permits to mould composite materials and thermosetting polymers [26].

Hot embossing: is a process that provides a film of thermoplastic material inserted into the mould, which is heated in order to soften the polymer. In a evacuated chamber the micro structured mould insert is pressed against the film with high pressure: the mould insert is filled by polymer and micro structures are replicated in details. After the mould is cooled down the insert can be removed and the part is formed [26].

Injection compression moulding: is a combination of hot embossing and injection moulding. In this process the melted polymer is injected by a screw into an almost closed cavity and pressed against the micro structures in the tool closing phase.

Thermoforming: is a particular technique used to form thin thermoplastic films. The film is inserted into the one-side-only micro manufactured mould, which is closed and evacuated. The film is pressed against the tool by a gas at high pressure, then cooled down and demoulded.

2. Micro injection moulding

Micro injection moulding is the technology that most assures a good quality resulting component and an easy manufacture process. It allows mass production with relatively low costs, has a short cycle time and a great potential for full automation. Moreover this technique provides accurate replication and dimensional control.

Advantages of micro injection moulding compared with other micro manufacturing techniques are the following [3].

(1) A wide range of thermoplastic polymers can be used (low viscosity formulations of standard polymers).

(2) The potential for full automated production cycle.

(3) Short cycle time.

(4) Relatively low costs for mass production.

(5) Accurate replication of micro features on mould structure.

(6) Good dimensional control of final product.

On the other hand, this production process has some limitations that need to be overcome before micro injection moulding fabrication of micro components can be realized in wide scale [57].

Principal disadvantages are defined by following elements.

(1) Mould and component design: there are limited allowed geometrical designs to ensure smooth demouldability, because of the end shape process nature.

(2) Performance of mould machine: optimization of process parameters is needed, in particular in case of high aspect ratio features, in order to produce qualitative acceptable components.

(3) Need of right material choice and processing conditions.

It is important to correctly design the mould in order to avoid problems during manufacturing phase: part dimensions and position and shape of parting line must be carefully projected. Moreover, also tolerance and surface finishing of mould cavity as well as undercuts and specific features have to be considered in mould design.

2.1. Injection moulding machine development. An injection moulding machine consists in four parts: plasticizing and injection unit, clamping unit, mould cavity and ejection system. Conventional injection moulding machines can be electric, hydraulic or hybrid, depending on their power.

With the aim of micro part production, all parts must be very accurate: positioning, movement and alignment of two mould half as well as linear and rotational precision of machine screw have to be ensured. With servo hydraulic systems this required accuracy is difficult to obtain, therefore servomechanisms of electrically driven machines can be used [55] and [60].

Whereas the identification of switch over point using injection pressure in traditional injection moulding machines is not accurate enough for micro scale,

micro injection moulding machines use injection plunger position to determine it [55].

Furthermore, because of the smaller sizes of tools required in micro injection moulding, the whole machine can present reduced dimensions compared to traditional injection moulding machines.

In the evolution of micro injection moulding machines from the macro ones, two different designs have been developed [55] and [60].

(1) First design descends directly from the simple miniaturization of macro injection moulding machines. For micro machines the screw diameter is typically smaller than 20 mm but down limited approximately to 12 mm, because the pellet needs to fit into screw channel and is characterized by a conventional size.

(2) Second design separates the units of plasticizing and homogenization from injection system. This design can be realized in two different ways: one provides usage of a plunger and a hot cylinder (as shown in figure 4), the other uses a conventional small screw and a barrel (figure 5). Generally screws provide a more homogeneous plasticization than plungers.

2.2. Injection moulding functioning. Injection moulding process, that happens in Micro Power 15 from Wittmann Battenfeld, consists in seven principal phases that can be summarize as following.

(1) Introduction of polymer pellet in the fixed extruder screw and plasticising in this heated barrel: screw is designed with a first feeding section, a consequent compression zone.

(2) Filling of metering chamber of injection unit.

(3) Enclosure of shut off valve to avoid polymer back flow.

(4) Push of the predefined melt polymer volume from the chamber into the injection barrel by plunger.

(5) Pressing of melt polymer in mould cavity by injection plunger.

(6) Holding pressure for a specific time to compensate material shrinkage. During cooling the polymer solidifies because of the mould temperature decreasing below glass transition temperature.

(7) Ejection phase thanks to extractor rods [3].

In order to obtain a complete replication of micro features before the material solidification temperature gradient between mould and melting polymer should be minimized. Therefore, in micro injection moulding mould temperature is higher than the one in traditional macro process and temperatures over glass transition temperature can be reached. The principal disadvantage consequent to mould heating is an increase of cycle time that could lead to a material degradation of the material located in the barrel [3] and [60]. Another consideration is about air vents in mould cavity: because of their dimensions similar to micro structures in mould cavity, they have to be evacuated with an external evacuation system in order to avoid defected inducted by compression.

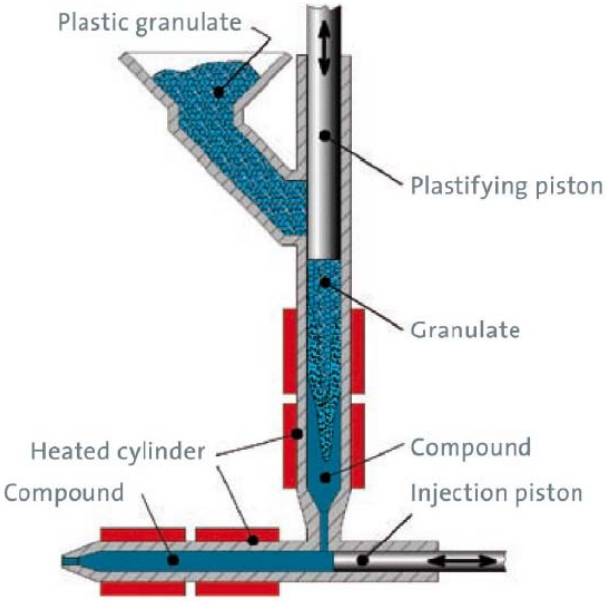

Figure 4. Design of injection system with hot cylinder and plunger. Plasticizing piston measures the right quantity of polymer and pushes it through the hot cylinder; injection piston fills the mould.

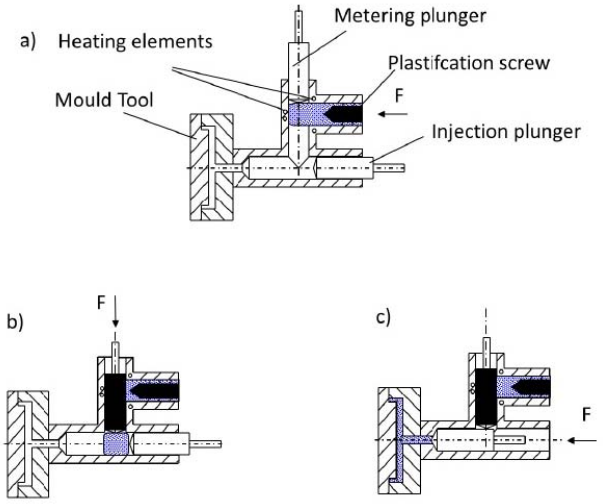

Figure 5. Design of injection system with screw and barrel, and functioning phases. Screw plasticizes homogeneously melt polymer (a), which is moved in a chamber (b) and then is pushed in the mould cavity by a plunger (c).

2.3. Process parameters affecting replication quality. The most efficient combination of injection moulding parameters has already been researched in many studies, and it has been shown that a single combination can not be found for all the possible materials. Process parameters affect differently various polymers, the following were found to be in general the most influential:

- mould temperature;
- melt temperature;
- injection speed;
- injection pressure;
- holding time;
- holding pressure; and
- cooling time.

In order to evaluate the replication quality some process responses have to be considered. In literature are reported the most important:

- filling quality of micro sized channel;
- feature dimensions;
- part mass;
- flow length;
- filling volume fraction;
- weld line formation;
- demoulding forces;
- mould cavity pressure;
- minimum injection time; and
- pressure and temperature distribution.

The different chosen responses of statistical studies can lead to different main results [2].

Chapter 2

Demoulding

Last step of injection moulding process consists in removing of finished part from mould cavity, when it is enough solidified to remain stable outside mould. This operation could influence component mechanical properties and should be executed in the most careful way possible.

With size reduction from macro to micro parts, possible sites in which locate ejection pins decrease. Moreover also the micro part itself becomes weaker and more damageable compared to macro parts, which are sufficiently rigid to tolerate ejection force without deteriorating themselves.

Various defect can be generated during ejection phase: in figure 6 are reported two examples of demoulded part defects for a component in Policarbonate (PC). This images demonstrates how the rods diameter can affect demoulding effects: with a larger ejection surface defects are smaller (but it also depends on material type) [24] and [22].

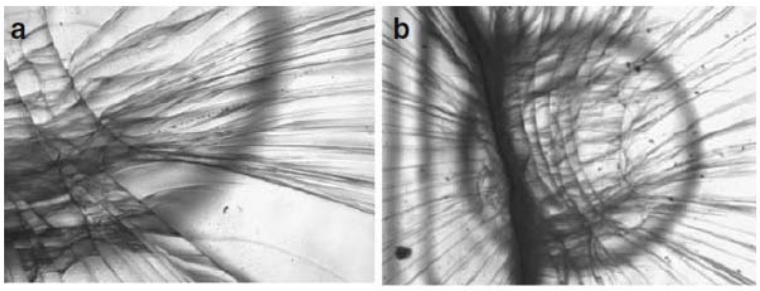

Figure 6. Demoulding defect on PC parts, on the left with 3 mm ejector pin and on the right with 1.6 mm.

During cooling phase both mould and polymer thermal contraction occurs, because of the different thermal expansion coefficients metal and plastic parts have

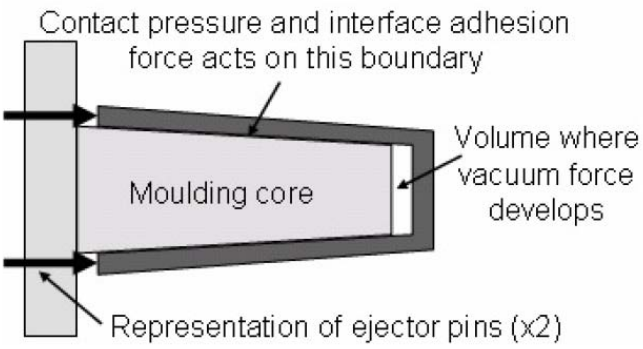

Figure 7. Demoulding scheme.

different contractions: in particular thermal expansion coefficient of metallic core is lower than the one of polymer. Thus, during shrinkage of thermoplastic polymer normal stresses around the core surface arise. In order to overcome this stresses at the part-mould interface, ejection rods have to apply a significant force at the part. This demoulding force is a parameter to consider during mould design and has to be minimized to avoid significant defects in the part. All other parameters that influence demoulding behaviour have to be studied to avoid part structural failure or deformations.

Stresses which develop in moulded part are strongly related to normal pressure and consequently to shrinkage, part stiffness and mould packing. A tangential force is required to overcome such normal forces effect and has to generate relative motion between part and tool during demoulding process [48]. Figure 7 shows a schematic demoulding example.

Demoulding forces increase for micro features with high aspect ratios (section 2), because of the wide contact area between mould and polymer [60]. Ejection system induces local forces on moulded part and their sum must exceeds holding forces which keep finished part in contact with mould moving part. In order to avoid damages (as core breaking) during detachment of polymer from mould, stress applied should not exceed material tensile yield stress: applied ejection force has to be confined in this range between holding forces and tensile yield stresses.

A usual ejection force system provides a series of ejector rods and each of them has to overcome the local friction force without introducing defects to removed part: part deformation is affected by pins number and position in mould cavity [24] and [32].

1. Demoulding friction models

Definition of demoulding force can be enunciated as the force necessary to start the ejection movement of the part without considering frictional effects of actual ejection mechanism.

The prediction of demoulding force could help in mould design, in order to do that several models have been proposed assuming the existence of an accurate

friction coefficient. Friction can be defined as resistance to relative motion offered by bodies in contact [48].

Ejection forces occurring during demoulding phase are representable with two type of friction coefficient.

(1) *Static friction coefficient*, that derives from shrinking of part on core and describes the initial breakaway motion stage.

(2) *Dynamic friction coefficient*, that occurs when part moves relatively to core surface [37] and [14].

In order to demould a part the static friction coefficient is the most important to consider because is the major between both.

From empirical Coulomb friction law derive most of mathematical models, that describe tangential force required in demoulding stage in order to overcome frictional forces.

[18] describe the release force (F_R) with Coulomb model:

$$F_R = \mu \cdot p_s \cdot A_p$$

where:

μ = dimensionless friction coefficient
p_s = surface pressure
A_p = involved surface

This surface can be determined for simple geometries by a qualitative consideration of part shrinkage. Local surface pressure is the result of part shrinkage and depends mostly on material and processing parameters. μ depends on several factors as material, mould surface roughness, moulding pressure, demoulding velocity and mould temperature.

Because of the difficult determination of friction coefficient and contact pressure, four alternative methods are following presented in order to permit estimation of ejection force.

(1) [35] develop a ejection force equation for a vented cylinder that is:

$$F_R = \mu \cdot E \cdot \Delta d_r \cdot s_m \cdot 2\pi L$$

where:

E = elastic modulus of thermoplastic polymer at ejection temperature
Δd_r = relative change in diameter of part immediately after ejection
s_m = part thickness
L = part length in contact with mould core

(2) [11] demonstrate that ejection force is affected by cooling time, surface finish, direction of polish and draft angle. The equation that descends from their study for a box shaped not vented part is:

$$F_R = \mu \cdot E \cdot \alpha \cdot (T_S - T_E) \cdot \frac{8 s_m L}{1 - \nu} + (W_1 W_2 p_A)$$

where:

α = thermal expansion coefficient
T_S = temperature at shrinkage starting
T_E = temperature at ejection instant
ν = Poisson ratio
W_1, W_2 = widths of rectangular core sides
p_A = atmospheric pressure

(3) [21] defines contact pressure (p_s) as:

$$p_s = \frac{\alpha(T_M - T_E) \cdot E}{\frac{1}{2t} - \frac{\nu}{4t}}$$

where:

T_M = temperature at softening point
t = part thickness

Therefore, ejection force results:

$$F_R = \frac{\alpha(T_M - T_E) \cdot E \cdot \pi L \cdot \mu}{\frac{1}{2t} - \frac{\nu}{4t}}.$$

(4) [29] develops a ejection force equation for hollow thin walled cones with a draft angle θ and considers vacuum forces:

$$F_R = \frac{2\pi E \cdot \epsilon \cdot s_m \cdot L}{1 - \nu} \cdot \frac{\cos\theta(\mu - \tan\theta)}{1 + \mu \sin\theta \cos\theta} + 10B$$

where:

ϵ = elastic strain
B = projected area of core surface in core axis direction

First part of multiplication refers to contact pressure and the second to friction force; last term represents vacuum force.

These various types to define the same concept show the difficulty to consider the whole amount of parameters that affect ejection force. In each specific case, the right model has to be used considering parameters that have a real effect on demoulding phase.

2. Parameters affecting demoulding force

As demonstrated in previous section, demoulding force is affected by several parameters: in this part are presented the most influential, such as properties of injected material, process parameters, mould structure and surface finish and dimensioning of actuation devices.

2.1. Actuation devices. In order to demould a finished part from the mould cavity, actuation devices are need. The most common situation provides usage of ejection pins that are economic and easy to install. Principal disadvantage of ejection rods lies in high local stresses and strains that these devices generate in part during ejection phase causing deformations and damages in solidified polymer [32]. Therefore, a proper layout and dimensioning of the ejectors has to be studied. However, micro components offer limited space for optimum positioning because of their reduced surface [24].

In order to determine size and layout of rods, [32] proposes a method that permits to minimize deformation and damage. This strategy first computes the ejection force needed to overcome friction between mould and part, second transforms this distributed force in an equivalent set of discrete forces. As third step both location and size of ejectors are determined in order to obtain these discrete forces. In their studies [4] observed that also ejector number affects stresses at mould-part interface, in particular a greater number of pins reduces stress distribution in moulded part.

Also mould design affects actuation device, in fact in [3] mould features placement is studied and the result is that demoulding forces increase when features are further from shrinking centre.

2.2. Aspect ratio. Mould design could influence both injection and ejection phase. A parameter that describes features geometry is the aspect ratio (AR). It is defined as the ratio between longer dimension and shorter one. In particular for geometries used in this study aspect ratios for mould cores and part channels are defined as follows:

$$AR_{\text{cores}} = \frac{\text{height}}{\text{diameter}} \quad \text{and} \quad AR_{\text{channels}} = \frac{\text{height}}{\text{width}}.$$

[3] suggest that the critical minimum dimensions which can be successfully replicated by injection moulding are mainly determined by size of structural feature aspect ratio as well as size of area covered with such structures.

Achievable aspect ratio is limited by a series of variables that are function of micro features geometry, their position, polymer nature and process parameters.

A physical effect directly linked with aspect ratio is hesitation effect, which is a phenomenon that occur when a polymer tends to easily flow into cavities with low resistance areas of greater cross section and consequently flow stagnates at the entrance of micro structures. The negative result is that polymer cools down quickly and does not fill the entire cavity. Micro features with an high AR have wide surface compared with volume, so higher cooling rates occurs [3] and [57].

Shear thinning effect can be described as a considerable heating due to viscous dissipation near cavity wall when high shear stresses are present. Viscosity of melt polymer decreases near walls and also thin walled parts with high aspect ratio can be filled.

2.3. Injected material properties. Another factor that influences demoulding stage is the orientation of injected polymer: a preferential orientation during injection phase leads to a certain shrinkage direction. Thus, in [3] is affirmed that

injection polymer path inside mould has to be considered for microfluidic substrate design.

During cooling phase, temperature changes and undergoes glass transition temperature. This leads to volume variations of the cooling polymer that are the result of shrinkage process. As previously explained this behaviour influences a lot ejection forces. A polymer shrinkage behaviour can be evaluated with commercial simulation programs, if the particular polymer is present in database.

2.4. Melt and mould temperatures. In [47] is affirmed that increasing injection temperature reduces shrinkage, because of the better pressure transmission. Conversely, [22] show that ejection force is negatively influenced by melt temperature after its maximum has been reached. Maximum ejection force is strongly dependant on moulding factors that enhance surface replication: higher injection temperature allow a minor polymer viscosity that leads to a grater friction due to polymer interlocking at mould interface. Melt temperature has to be balanced between these two aspects.

In order to avoid high interlocking problems, in micro processes high mould temperature is adopted: it is usually set over glass transition temperature. In this way filling ratio is improved and replication of micro features is favoured. Increasing of mould temperature reduces ejection force.

2.5. Packing pressure. With the aim of decreasing demoulding forces, an high holding pressure and a long cooling time are required. In their study, [22] found that a direct correlation between ejection forces and holding pressure. They show that a excessive increasing of pressure leads to a great ejection force that needs to be applied for a long time, this increment produces an higher risk of damages and deformations due to higher stresses induced in part.

Other studies ([42] and [28]) conclude that shrinkage is affected by packing pressure. In addiction, [47] affirms that an higher holding pressure reduces part shrinkage in all directions. As for other parameters, the optimum value lies in the middle in balance between disadvantages provide by excesses in both directions.

2.6. Injection speed. Generally in micro injection moulding, a great injection speed is preferable in order to avoid early polymer solidification due to rapid cooling in mould. An high injection speed does not influence directly ejection force value, but it is important to obtain a close replication of micro features and a complete cavity filling.

For micro injection production, high process parameters are advantageous in the limit of replication fidelity and polymer dimensional stability. However these parameters must be superior limited to avoid affection of demoulding phase. In order to obtain the best result in terms of high performance process and high quality moulded part, theoretical best value for all injection parameter has to be found for each specific case.

2.7. Influence of superficial roughness. In literature has been observed that generally ejection force decreases with decrement of mould surface roughness. But the opposite effect can be found is nano structures or highly polished surfaces are used

[52] and [48]. At least, from this study can be observed that in order to minimize demoulding force a optimal surface roughness exists.

In figure 8 the effect of different surface roughness levels on ejection force, for various materials are reported from [52]. In case of Polypropylene (PP) demoulding forces decrease with increase of surface roughness until the values reaches 0.2 µm. After this value ejection force starts increasing as long as roughness increases. Analogous graph is for Poly(methyl methacrylate) (PMMA): demoulding force decrease until roughness of 0.092 µm is reached, then it rises up to an Ra value of 0.689 µm. The same plot generated for Polyethylene terephthalate (PET) presents an almost straight decrement of ejection force until Ra is 0.026 µm, then it decrease slowly to 0.212 µm and slowly rises till 0.689 µm. These graphs clearly show the existence of an optimum roughness value for each material.

Conclusively ejection force highly depends on mould surface, and in order to minimize roughness effects on demoulding phase a common practice is to produce a surface finishing in ejection direction.

2.7.1. *Roughness parameters.* Principal parameters that should be investigated in order to determine roughness properties of a certain acquired profile are the following.

Ra: arithmetic mean deviation of the assessed profile: defined on the sampling length. Ra is used as a global evaluation of the roughness amplitude on a profile and is meaningful for random surface roughness machined with tools that do not leave marks on the surface, such as sand blasting, milling, polishing.

Rp: maximum profile peak height: height of the highest peak from the mean line, defined on the sampling length.

Rv: maximum profile valley depth: depth of the deepest valley from the mean line, defined on the sampling length.

Rz: maximum height of the profile: defined on the sampling length. Rz parameter is frequently used to check whether the profile has protruding peaks that might affect static or sliding contact function.

Rk: core roughness depth.

Rpk: reduced peak height. This parameter is used to characterize protruding peaks that might be eliminated during function.

Rvk: reduced valley depth. This parameters is used to characterize valleys that will retain lubricant or worn-out materials.

Sa, Sp, Sv, Sz, Sk, Spk, Svk correspond to the previous parameters, when estimated for a surface and not for a profile.

The Abbott-Firestone curve describes the surface texture of an object; mathematically it is the cumulative probability density function of the surface profile's height and can be calculated by integrating the profile trace. This curve is used to estimate hills and valleys and is directly linked to Spk, Svk, Rpk and Rvk.

2.8. Superficial coatings. Surface coatings can be a valid alternative to reduce demoulding force, because they can fill cavities and sooth wrinkly surfaces and

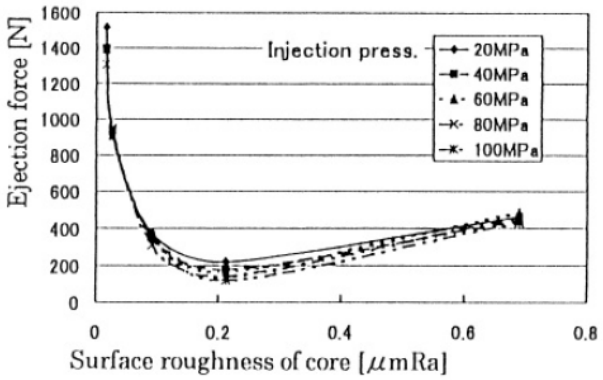

(a) *PP*.

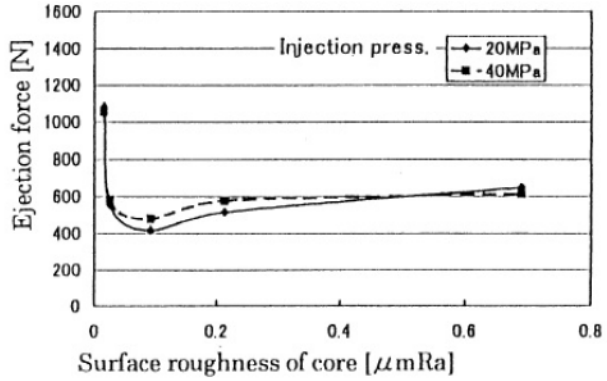

(b) *PMMA*.

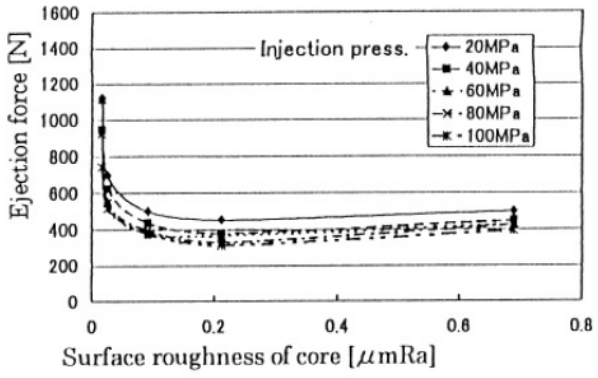

(c) *PET*.

Figure 8. Relation between ejection force and surface roughness for different polymers.

also own chemical properties that can influence demoulding phase. These chemical properties of coating materials can ease or make more difficult extraction process: it is important to consider the specific combination of coating material and injected polymer.

Coatings can be produced by many techniques as Physical Vapor Deposition (PVD), Chemical Vapor Deposition (CVD) or Pulsed Laser Deposition (PLD) in this way resistance of tool surfaces is improved and part-mould forces are reduced.

[25] investigate different behaviours of treated and untreated tools. Surface treatment chosen is DLC, and two materials are tested for injection moulding. Average demoulding forces measured for both polymers permit to conclude that surface treatments significantly reduce the extraction force in comparison with untreated tools. As noticed by [12] also polymer nature can affect the results in term of work energy necessary to eject part from insert.

[44] observed that ejection stage is divided in a static phase (unsticking) and a dynamic phase (dynamic friction). This study shows that amorphous polymers are sensitive only to unsticking; whereas for a semi-crystalline polymer, which has a higher shrinkage, contribution of dynamic friction is more relevant and friction value behaviour has no transition between unsticking and dynamic friction steps. For both polymer types it has been noticed that coatings influence ejection force as of their thermal properties, roughness and physical adhesion of polymer on surface. Consequently, in case of coated mould couple polymer-coating is the parameter that mostly influences the demoulding force value.

3. Mould wettability

The aim of this study was to understand how different materials interact with various surface coatings, so the most interesting zone to analyse is the interface between mould and polymer during ejection phase. In order to do that, wettability of coated mould was investigated.

Wettability is the capability of a liquid to partially or completely wet a surface where is deposed. The only physical parameter necessary to define this property is contact angle between liquid drop and surface that is consider infinitely wide and plain [20], [6], [7] and [8].

Contact angle depends directly on surface properties as finish and material. Considered system consist in three physical phases: surface is solid, drop is liquid and atmosphere is gas. Between each phase there is a separation surface, at each interface a stress belong. Figure 9 represent a schematic example of stress distribution: γ_{SL} is stress at solid-liquid interface, γ_{SG} lies at solid-gas interface and γ_{LG} represents stress between liquid and gas, its direction is tangential to drop profile in contact point.

Contact angle can be determined considering these stresses by:

$$\cos\theta = \frac{\gamma_{SG} - \gamma_{SL}}{\gamma_{LG}}.$$

If a liquid is required to spread over solid surface, is necessary that its surface stress does not exceed solid surface stress. Vice versa if the liquid should wet less

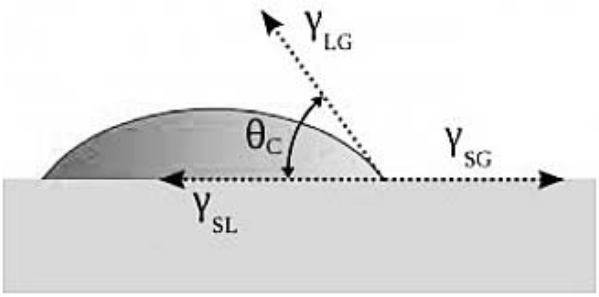

Figure 9. Drop of liquid on a plain and schematic representation of surface stresses, θ is the contact angle.

solid surface, its surface stress must be higher than the solid one.

Solid surface free energy can be divided in three categories.

(1) Materials with high surface free energy present strange atomic bonds of chemical type (covalent, ionic and metallic). Polar liquids are able to completely wet an high energy surface.

(2) Material with low surface free energy present weak molecular bonds of physical type (Van der Waals and hydrogen bond). These surfaces allow partial or complete wetting depending on liquid nature.

(3) Material with extremely low surface free energy are usually polymers and fluoromaterials.

In this study coatings belong to the second category, and the contact angles have been estimated for several combinations of polymer and coating.

3.1. Viscosity. Viscosity is a fundamental property of injected material, because leads mould filling phase. If a polymer presents an higher viscosity filling operations result more difficult and micro features could not be replicated as required. In order to make less viscous a polymer temperature is increased.

William-Landel-Ferry model can be used to predict the effect of temperature on viscosity. The WLF equation is used for polymers that have a glass transition temperature. The model is:

$$\eta(T) = \eta_0 \exp\left(\frac{-C_1(T - T_r)}{C_2 + T - T_r}\right)$$

where:

T = variable temperature
T_r = experimental parameter linked to glass transition temperature
η_0, C_1, C_2 = empirical parameters obtained through regression to experimental data

This method is useful because permits to easily predict the viscosity value at the melting temperature used during experimental process.

Due to their large molecular mass, polymers used in injection moulding process are viscoelastic materials, that means they perfor. Elastic materials return quickly to their original state, when stresses are removed. Viscoelastic materials presents characteristics of both cases, therefore they exhibit time dependant strain.

In case of injection moulding technology, a melted polymer that flows into a cavity channel of thickness t with average speed of v_{av} is characterized by a mean shear rate ($\dot{\gamma}_{av}$) and a shear stress (τ), that represents the resistance to deformation, which are respectively:

$$\dot{\gamma}_{av} = \frac{2v_{av}}{t} \quad \text{and} \quad \tau = \eta \cdot \dot{\gamma}.$$

η is the melted polymer viscosity and varies with material and temperature as described by WLF model. This property can be defined as material internal resistance to deformation, and mathematically as:

$$\eta = \frac{\tau}{\dot{\gamma}}.$$

Part 2

Experimental setup

Chapter 3

Materials

In order to study interaction between injected material and mould coating, four polymer were selected.

The main difference between the principal categories of polymers (thermoplastic and thermosetting polymers) has to be researched in their molecular structure. Thermoplastic materials are characterized by polymer chains associated with intermolecular forces, which, becoming weaker at the increasing of temperature, lead to a viscous liquid. Therefore thermoplastics can be reshaped by heating. On the other hand, thermosetting polymers derive from a prepolymer in a viscous state that changes irreversibly into an infusible and insoluble polymer network by curing process.

Chosen materials are all thermoplastic polymers, so they are characterized from a glass transition temperature and a melting point. When the temperature sets between these values physical properties of the material change without being associated to a specific phase change. Thermoplastic polymers become mouldable and can be processed by injection moulding, then they solidify upon cooling.

The main partition in thermoplastic category has to be seek in molecular structure, which can be amorphous or semi-crystalline. In the first case polymers appear transparent and in the second case they are matt. Amorphous polymers present twisted chains, instead semi-crystalline polymers have ordered chains in the same orientation, interspersed with amorphous zones.

1. Characteristics of materials

Two of the selected polymers are amorphous: Polystirene (PS) and Cyclic Olefin Copolymer (COC); the other two are semi-crystalline: Polyoxymethylene (POM) and Polyamide (PA). In particular the used material are:

- Total, PS Crystal 1540;
- Basf, POM Ultraform H2320;

Table 1. Physical properties of different polymers.

Property	PS	POM	PA	COC
Chemical formula	$(C_8H_8)_n$	$(CH_2O)_n$	$(C_6H_{11}NO)_n$	$(CH_2)_n - (CH)_n$
Structure	Amorph.	Semi-cryst.	Semi-cryst.	Amorph.
Transition temp. (°C)	100	145	230	134
Ejection temp. (°C)	86	110	180	200
Melt temp. (°C)	235	200	280	260
Elastic mod. (MPa)	3200	3200	3100	3200
Dehumid. (°C × h)		90×2	80×3.5	80×6

- Basf, PA6 Ultramid B40 LN; and
- Topas, COC 5013L-10.

The choice of these particular materials was lead by their high flow ability, that makes them suitable for micro injection moulding applications.

1.1. Physical properties. Main properties of selected materials are reported in table 1. It is important to notice that three polymer of four need to be dehumidified: presence of humidity in injected material could affect negatively final resulting part, because at the melting temperature water withheld in processing polymer evaporates producing bubbles and awaking the final demoulded piece.

An important physical property to take in consideration is viscosity. To determine the variation of polymers viscosity in function of shear rate and temperature a rotational rheometer (TA Instruments, ARES) and a capillary rheometer (Ceast, Rheo 2500) were used.

In plot 1 correlation of viscosity and shear rate is represented for different temperatures. The trends are similar, but it is clear that, with an higher temperature (T), viscosity (η) decreases at same shear rate value (γ).

Moreover plot 2 shows the variation of specific volume (v_s) with temperature, at different pressure (P) levels. An higher pressure determines a lower specific volumes, that means a higher density ($\rho = v_s^{-1}$).

In order to compare the rheological behaviour of different material a WLF-model was fitted to the experimental data. In plot 3, for each material the viscosity value estimated at different temperature and for a fixed shear rate of $200\,s^{-1}$ is reported.

From plot 3 can be noticed that PS and COC have the lowest values of viscosity at the considered temperatures, on the other hand POM and PA are more viscous at the same temperatures. This behaviour can be related to the molecular structure of polymers, in fact PS and COC are amorphous structured, POM and PA are semi-crystalline instead. This analysis leads to the conclusion that PS and COC can replicate topography of mould surface better than POM and PA, thanks to their low viscosity.

Table 2. Injection moulding parameters employed for each polymer.

Parameter	Unit	PS	POM	PA	COC
Melt temperature	°C	240	235	240	265
Mould temperature	°C	60	80	70	100
Injection speed	mm/s	200	200	200	200
Packing pressure	bar	150	150	150	150
Switch over	bar	690	640	700	720
Dosage	mm^3	64.8	67.7	62.8	66.7
Cooling time	s	6	6	6	10
Ejection velocity	mm/s	10	10	10	10
Extractor displacement	mm	3	3	3	3

1.2. Injection parameters. The right choice of injection moulding parameters depends on several factors, first of all it is important to consider the correlation between each others. As shown in previous section (section 1.1) both temperature and pressure influence viscosity, that is the principal indicator to take in consideration for a good injection process.

The variation of each injection parameter produce an evident effect on the moulded result. In order to compare resulting ejection forces, a fixed combination of injection moulding parameters was adopted. The only exceptions are melt temperature and mould temperature, which were chosen coherently with materials data sheets. Proper values of temperature mean that small variations of dosage and switch over are necessary to maintain the same final result. Table 2 summarizes the effective injection moulding process parameters.

2. Wettability tests

In order to estimate the wettability of selected polymers, the contact angle at the interface between melted polymer and coated surface was evaluated. The behaviour of each polymer on different coatings was monitored at the melt temperature adopted for injection moulding processes (PS at 240 °C, POM at 235 °C, PA at 240 °C and COC at 265 °C).

Experimental setup used to lead this kind of tests consist in:

- chamber with electrical heating system;
- thermocouple to control chamber temperature;
- high speed camera;
- light source; and
- image analyser.

The experimental procedure can be summed up in five steps.

(1) Heating of the empty chamber at the correct melt temperature.

(2) Positioning of the coated surface specimen and waiting for its thermal equilibrium.

(3) Placement of a weighted piece of polymer.

(4) Acquisition of images to record the wetting behaviour of melting polymer.

(5) Analysis of contact angles.

Images of melting polymers were acquired at 25× of magnification with the high speed camera, the acquisitions continued for 10 min with a recording step of 30 sec.

Edge detection algorithm associated with Canny method was utilized to obtain a image segmentation starting from acquired photographs. This MATLAB® algorithm is an image processing technique used to determine the boundaries of objects within images. It works by detecting discontinuities in brightness, that was why a back light source was used. It permits to describe the polymer drop by fitting its contour with a straight line at the base and an half ellipse at the curved profile. Than left and right contact angles were estimated.

For each combination of melting polymer and surface coating, three measurements were executed in order to obtain a standard deviation.

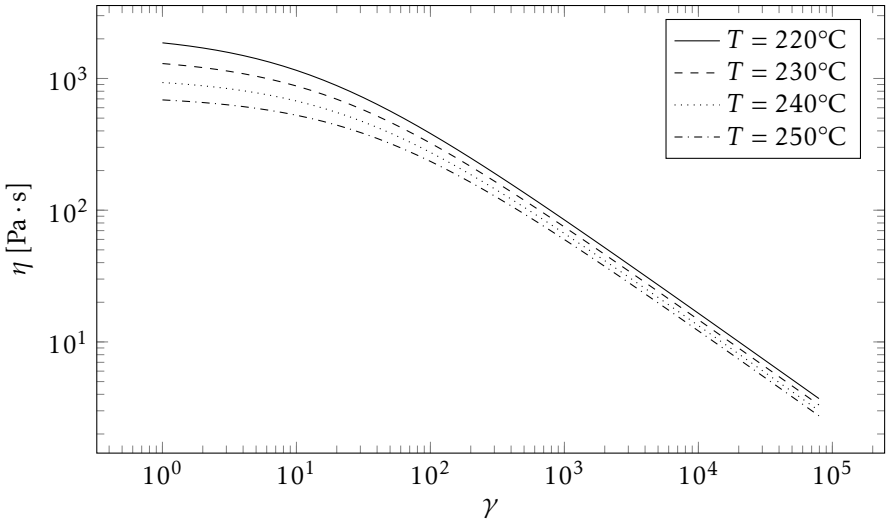

Plot 1. Trends of PS viscosity at temperature variation, correlated with shear rate.

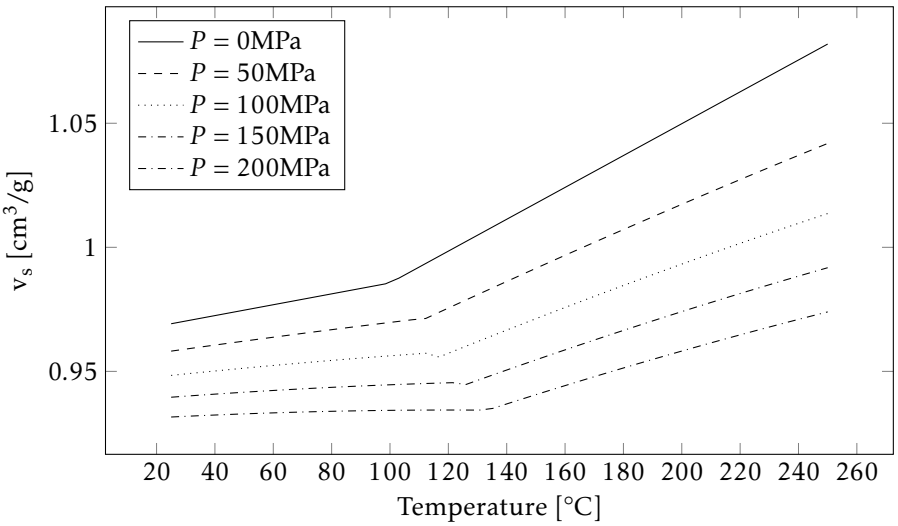

Plot 2. Trends of PS specific volume variation in function of temperature and pressure.

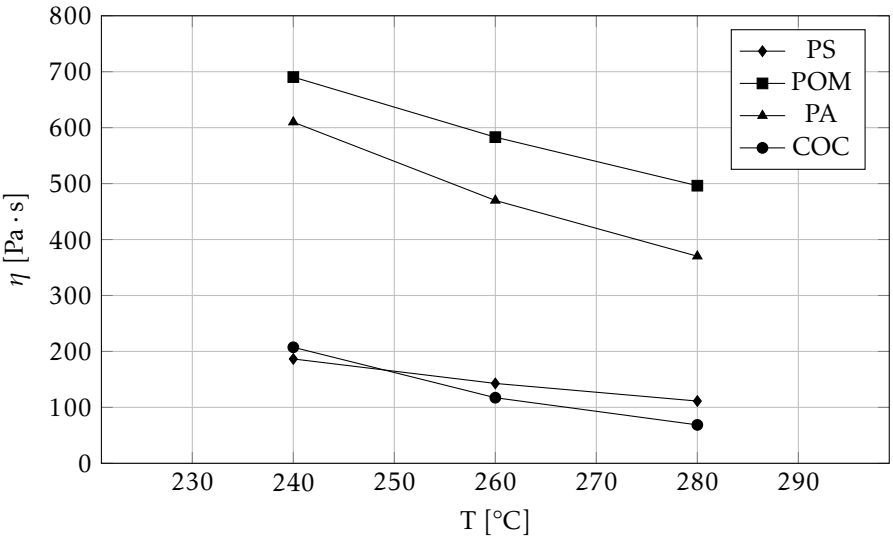

Plot 3. Trends of material viscosity at temperature variation.

Chapter 4

Mould production

Because of the reduced dimensions of the micro parts, moulds should be accurately designed and manufactured and a particular attention to the tolerance should be made. In order to obtain metrologically acceptable micro components, high performing technologies should be used: in this chapter micro Electrical Discharge Machining (μEDM) and micro milling are presented.

1. Mould cavity description

Moulds fabricated for injection moulding process are always constituted of minimum two parts: a fixed part and one or more moving parts. The specific mould

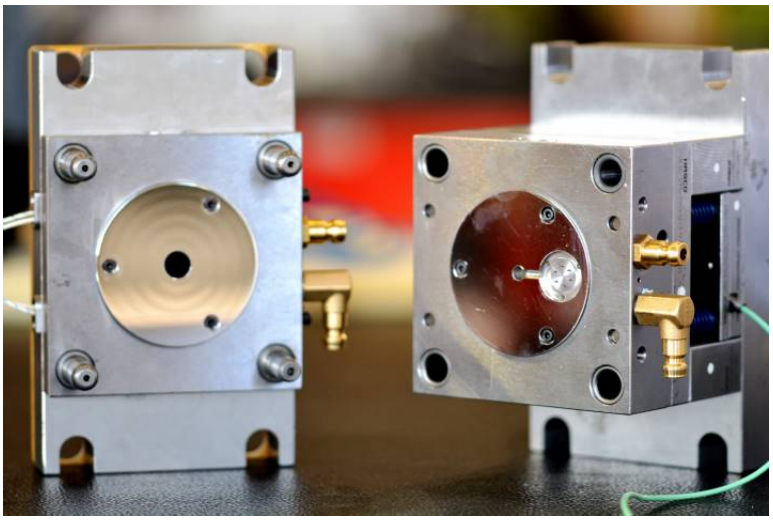

Figure 10. Fixed part of the mould on the left and moving part on the right.

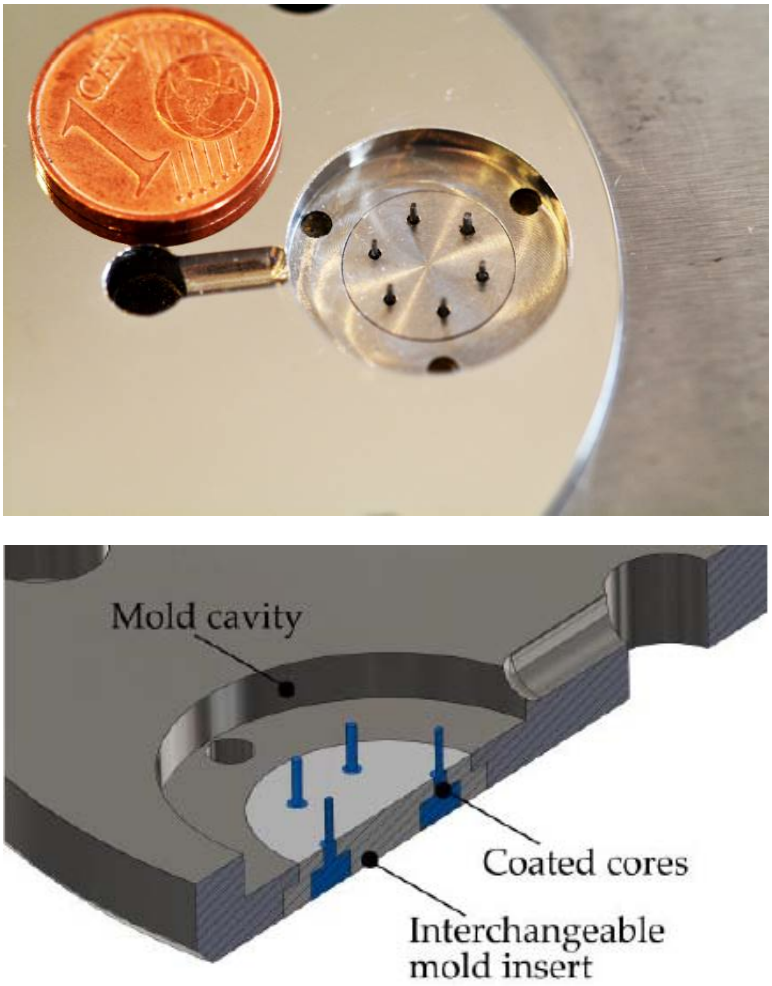

Figure 11. Mould cavity.

used in this study is composed of a fixed plain part and a moving part mounted on a rotating plate: it can be seen in figure 10.

Contact area between two parts of the mould is equal to 95 mm × 95 mm. Mould cavity is shown in figure 11 and can be described as a cylinder with a diameter of 18 mm and height of 2 mm, with total volume of 565.5 mm^3. In the centre of the cavity a interchangeable mould insert takes place, it is fixed in the cavity by a shrinkage fit. This removable plate permits to switch from a configuration to another: different cores set can be easily exchanged, and only a mould

is necessary for all the coated cores used in this study. The replaceable inserts minimize mould manufacturing costs and increase mould versatility.

The mould insert is characterized by six through micro holes with a diameter of 400 µm, that are located at the vertices of a centred regular hexagon with 3.5 mm of side. All dimensions are reported in figure 12.

The principal reason why the mould was conceived with these particular features is that the design represents a typical example of multilayer microfluidic device. In this way isolation of the effect of mould cores surface properties on demoulding force is allowed.

Six standard Hasco® ejectors with diameter of 800 µm were used to produce a single set. Four identical sets were manufactured, in order to produce the different coated mould inserts. Ejectors were cut and smoothed by EDM technology, then machined by micro milling to obtain the desired geometry, reported in figure 13.

2. Micro Electrical Discharge Machining - µEDM

Electrical Discharge Machining is a thermoelectric process that erodes material from the processing piece by high frequency discrete sparks between the piece itself and the electrode tool, both submerged in a dielectric fluid. These sparks remove continuously the material from piece surface through melting and evaporation: to correctly work, piece and electrode should be separated by a specific gap called spark gap. During the process the dielectric fluid acts as a deionising medium between electrode and manufacturing part, moreover its flow evacuates the resolidified material debris from the gap. Any electrical conductive material can be machined by EDM. In general, this technology permits to shape complex structures with high machining accuracy.

µEDM technology, at current state of art, can be divides in four categories.

(1) Micro-wire EDM (also micro Wire Electrical Discharge Grinding (µWEDG)), where a wire of diameter down to 0.02 mm is used to cut through a conductive workpiece.

(2) Die sinking µEDM, where an electrode with micro-features is employed to produce its mirror image in the workpiece.

(3) µEDM drilling, where micro electrodes of diameters down to 5 mm are used to drill micro holes in the workpiece.

(4) µEDM milling, where micro electrodes of diameters down to 5 mm are used to produce 3D cavities by adopting a movement strategy similar to that in conventional milling.

On Sarix SX-200, presented in figure 14, ejectors were cut and leveled.

Technology used to shape cores is WEDG; the functioning is presented in figure 15. The workpiece rotates and is moved up and down, the wire electrode passes by with a very low speed and can be considered motionless in comparison with the rotating piece. Ejectors were cut at an heigh of 2.8 mm using a fast

technology (TEC 206), then the heads were leveled with technology TEC 105; process parameters of both technologies are reported in table 3. Figure 16 shows an instant during leveling manufacture.

3. Micro milling

In order to shape cores as described in figure 13, milling technology was used. The Kugler Micromaster 5X (figure 17) allows both 3 axes and 5 axes manufacturing: in this case 3 axes configuration was necessary.

Vertical mill process requires a spindle axis vertically oriented that holds milling tools. Tools rotate on the spindle axis and work on the piece in different ways depending on the chosen cutting strategy. In particular the process used to mill cores is external circular ramping: the tool rotate around the cut and leveled ejection rod reducing its diameter from 800 µm to 400 µm. In figure 18 appears an instant of this process on a pin.

To allow a proper adhesion of coatings to the steel core substrate, roughness parameter Ra had to be minor than 0.2 µm. Thus, optimal milling process parameters were researched as like as the best cutting strategy.

3.1. Influence of milling process parameters on roughness. Figure 19 represents a schematic vision of external circular ramping on the right and illustrates specific cutting parameters for this technology.

Principal cutting parameters to consider in order to obtain the best surface texture result are reported in table 4. Among these parameters, rotation per minute (n), feed per tooth (f_z), depth of cut (a_p) and cutting speed (v_c) are the most influential on surface finishing.

To completely define a cutting strategy four parameters are fundamental: v_c, v_f, n and f_z. If two of these four parameters are known, the other are determined thanks to the following equations:

$$v_f = f_z \cdot n \cdot Z_c$$

$$v_c = \frac{D_{cap} \cdot \pi \cdot n}{1000}$$

$$n = \frac{v_c \cdot 1000}{\pi \cdot D_{cap}}$$

$$f_z = \frac{v_f}{n \cdot Z_c}.$$

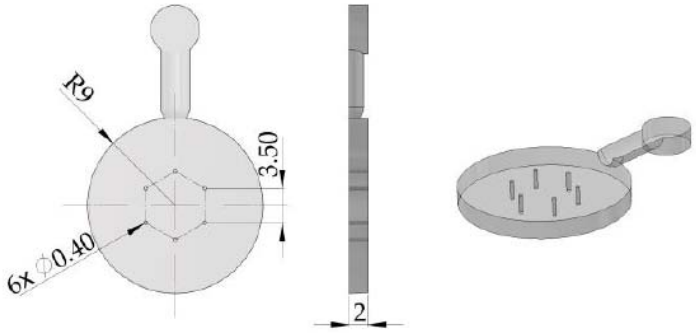

Figure 12. Part description.

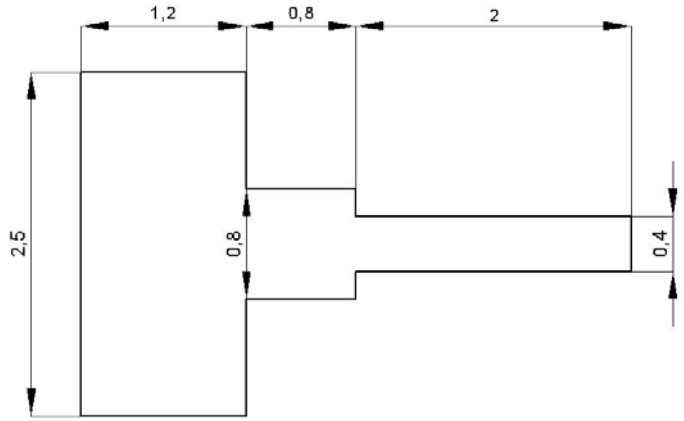

Figure 13. Core design.

Table 3. EDM parameters used for cut (TEC 206)and leveling (TEC 105) operations.

Parameters	TEC 206	TEC 105
Width	5	4
Frequency (kHz)	130	150
Current	50	80
Voltage (V)	130	110
Gain	1500	9
Gap	65	90
Energy	206	105

Figure 14. Sarix SX-200.

For the specific manufacture two other parameters can be geometrically defined starting from known values:

$$a_e = \frac{D_w^2 - D_m^2}{4(D_m + D_{cap})}$$

$$\beta = \arccos\left(1 - \frac{2a_e}{D_{cap}}\right).$$

Superficial texture is influenced by the combination of these parameters, the result can be very similar between strategies that use different values combinations. To estimate profile roughness value relative to different parameters combination without leading physical experiments following equation were used:

$$Ra = 1000\frac{f^2}{18\sqrt{3}\cdot r_e} \quad \text{and} \quad Rt = 1000\frac{f^2}{8r_e}$$

where:

$f = f_z \cdot Z_c$
r_e = tool cutting radius (0.002 mm).

It is important to notice that these equations are defined by [43] in case of turning technology: the values are to be considered an indication of the quality of chosen combinations.

3.1.1. *Test for optimal milling process parameters.* With the aim to obtain the best surface texture for coatings adhesion, three strategy were analysed.

(1) High speed technology uses a single cut, therefore the tool works with a large portion of lateral sharp.

(2) Z-constant strategy provides more than one cut at different z levels.

(3) Helicoidal process, in which the tool descends along z axis describing a spiral around the piece with tight step.

Figure 20 compares these three different technology approaches.

In table 5 parameters of the specific strategies just described are summed. They are always the same for each strategy, in order to directly compare the strategy and not the parameters combinations.

A qualitative analysis was conduced using SEM (see section 5.2). Comparative images taken at 1000× magnification are collected in figure 21: first image from left represent the case of high speed manufacture, the second shows z-constant strategy and the third is the result of a helicoidal process. In the first case a visible defect can be noticed on the lateral surface: this continuous slot is due to the hard entrance of the tool at the process beginning, thus this approach leads to a very bad result. The second strategy is better than the previous and at regular intervals presents visible grooves that are product by the several entrances of the tool during processing. At least helicoidal approach improve surface quality thanks to the slow and precise manufacture: no tool sign is visible.

The qualitative analysis between strategies leads the choice on helicoidal approach. At this point best milling parameters combination has to be researched. Following the indications provided by 3.1 three combinations return the same values for Ra and Rt: selected parameters sets are reported in table 6. Also the time required by the approach is written.

According to ISO-25178 and ISO-4287 the main surface roughness parameters were evaluated and reported respectively in table 7 and table 8. Two corresponding plots (plot 4 for ISO-25178 and plot 5 for ISO-4287) were generated in order to easily compare the tested combinations.

Table 7. Average values (A.V.) and standard deviation (S.D.) of surface roughness parameters evaluated according to ISO-25178.

ISO-25178								
Test	Sa (µm)		Sp (µm)		Sv (µm)		Sz (µm)	
	A.V.	S.D.	A.V.	S.D.	A.V.	S.D.	A.V.	D.S.
1	0.16	0.04	1.23	0.31	1.39	0.34	2.62	0.36
2	0.17	0.02	1.30	0.66	1.96	1.03	3.25	1.69
3	0.31	0.15	2.52	0.53	2.93	0.82	5.46	1.35

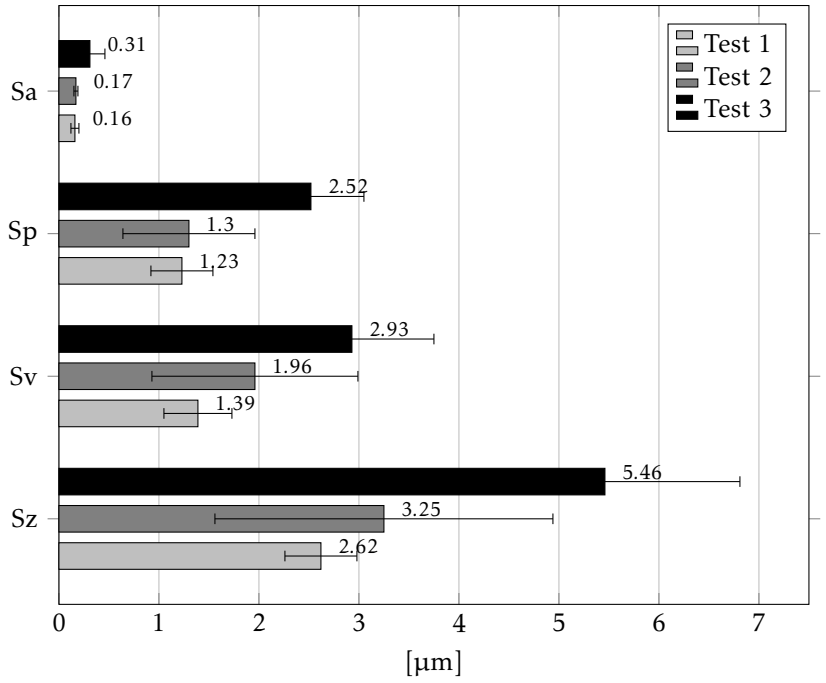

Plot 4. Surface roughness parameters evaluated according to ISO-25178.

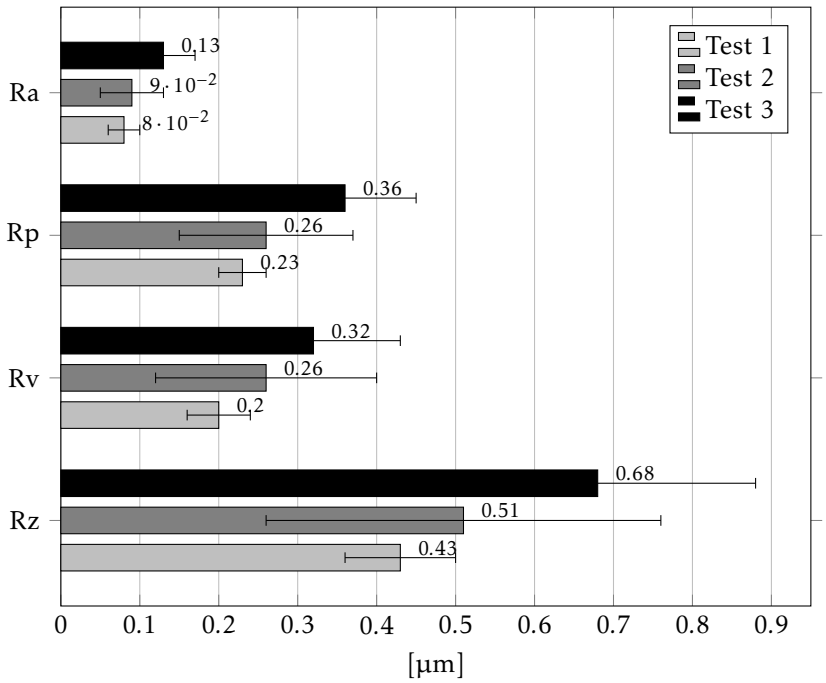

Plot 5. Profile roughness parameters evaluated according to ISO-4287.

Table 8. Average values (A.V.) and standard deviation (S.D.) of profile roughness parameters evaluated according to ISO-4287.

ISO-4287								
Test	Ra (µm)		Rp (µm)		Rv (µm)		Rz (µm)	
	A.V.	S.D.	A.V.	S.D.	A.V.	S.D.	A.V.	D.S.
1	0.08	0.02	0.23	0.03	0.20	0.04	0.43	0.07
2	0.09	0.04	0.26	0.11	0.26	0.14	0.51	0.25
3	0.13	0.04	0.36	0.09	0.32	0.11	0.68	0.20

In conclusion of this analysis *Test 1* was selected, this means that a top-down helicoidal approach with an axial depth of cut of 0.01 mm (a_p) was adopted. Machining operations were performed using bull nose tools (Kyocera, 1625) with a 0.7 mm cutting diameter (D_{cap}). Cutting speed (v_c) was set at 44 m/min, with a feed per tooth (f_z) of 0.001 mm.

Data sheets of tool and ejector pin used for this study are reported in appendix C and D.

4. Coatings

This study proposed to analyse the behaviour of various polymer during ejection phase of injection moulding process with different coated moulds. Selected coating materials are DLC-1, DLC-2 and CrTiNbN. In figure 22 are shown four representative cores, one per set: the first on the left is starting uncoated pin obtained by micro milling. The second and the fourth are DLC coated and appears black coloured because of the presence of Carbon; the third is coated with the metallic alloy CrTiNbN and present a shiny gold aspect.

4.1. Coatings characteristic. Coatings properties are reported in table 9.

Main difference between DLC and CrTiNbN lies in the different deposition technologies: Plasma Assisted Chemical Vapor Deposition (PACVD) for DLC and PVD for CrTiNbN.

PVD: is a technology used to produce thin films of coatings over the object surface, that can be process with different vacuum deposition methods. Generally the coating material passes from a condensed phase to a vapour phase and then back to film condensed phase. Sputtering and evaporation are the most common method to improve PVD. This process is very useful in micro application, because permits to reach all surfaces even in complex small geometries. The main negative aspect is that sputtering and evaporation cannot be easily controlled, so the coating can present agglomerates that cannot be avoid in deposition phase.

PACVD: is another technology used to deposit thin films of coating on a substrate. The material that has to be deposited is used in its gas state, after deposition it becomes solid. In this process are involved chemical reactions, which occurs after creation of a reacting gasses plasma. Plasma

is created by a discharge between two electrodes, where the dielectric is represented from the reacting gases. The major benefit of using PACVD instead of CVD is that the discharge creates electrons that are more mobile than ions, and the flux of electrons flows easily from plasma to the object surface. Surface will efficiently coated even if it is very small or complex. The other advantage of this technique is the lower temperature required for deposition, in fact electrons are so light that energy exchange between them and neutral gas is almost inefficient. Thus electrons can be maintained at high temperature, which makes them faster, and the neutral atoms can remain at ambient temperature.

Another difference between DLC and CrTiNbN coatings is that DLC is a multilayer instead of a bilayer as CrTiNbN: that is due to the technology used (paCVD) and to the material nature, in fact Carbon tends to create a layered molecular structure. In figure 23 is shown a damaged coated surface and a layered structure can be easily noticed. This property allows the deposition of a thicker coating in comparison with CrTiNbN.

DLC coatings consists of a highly networked hydrocarbon matrix with an high mount of sp^3 type bonds comparable to the diamond crystal lattice. The difference between DLC-1 and DLC-2 is the selected adhesion layer: Cr improves better than CrN the surface finish. Typical coating thickness lies in the range of 1-10 µm; in comparison with classical PVD hard coatings (for example TiN), the DLC coating is characterized by an increased elasticity and a comparable hardness.

5. Surface characterization

With the aim of surface characterization two instruments were used: an optical profiler and a Scanning Electron Microscope (SEM), the first generated quantitative results about surface topography and the second permitted to qualitatively estimate core surfaces.

5.1. Optical profiler. In order to quantify the roughness parameters that characterize three-dimensional surface topography of a sample, an optical profiler can be used.

The profiler is a confocal microscope that acquires a sequence of confocal images through the objective depth of focus and produces optically sectioned images of the sample. The topography can be evaluated for each images pixel by correlating the heights of signals collected through the sequence of images.

The Sensofar Plu neox showed in figure 24 and experimentally used for this study is a laser scanning microscope that produces a structured illumination pattern and, as other confocal microscopes, acquires reflected or backscattered light. In the particular configuration of a laser scanning microscope, a pinhole is located on the field diaphragm: the smallest illuminated spot is achieved on the objective focal plane and is typically a diffraction-limited spot. The reflected light passes back through the objective and is collected onto a second pinhole (confocal aperture) placed in the illumination pinhole conjugate position. A photo detector located at the rear of confocal aperture records the reflected signal. The signal on

photo detector is high when the surface is exactly placed on objective focal plane; conversely with a surface placed away from the focal plane the confocal aperture filters out noise and photo detector records a lower signal. Figure 25 represents the schematic functioning of a laser scanning microscope.

Each pixel of acquired images belonging to scanner sequence along z axis contains a certain signal value called "axial response similar". Different pixels have the axial response maximum located on different z axis positions according to the 3D surface shape. Mapping the z coordinates the 3D surface is reconstructed.

The instrument was used in confocal mode with 20× and 100× objectives and main characteristics are reported in table 10.

To acquire a significant image right scanning parameters should be chosen following the procedure.

(1) In bright field mode, point the profiler at the beginning of the area that has to be scanned.

(2) move the 20× objective along z axis in order to reach the focus position, then repeat the operation exchanging objective from 20× to 100×.

(3) Adjust the light level to minimize the returning noise during acquisition.

(4) Passing in confocal mode, set the amplitude of scanning in z axis direction.

Each core surface was analysed scanning four different lateral areas. For acquisition stitching method was used, hence six consequent images were acquired and together merged. Thanks to this method the resulting scanned area is longer than the one obtained with a single image.

5.2. Scanning Electron Microscope - SEM. The SEM can produce extremely detailed images of the surface of an object by scanning it with a focused electrons beam.

Figure 26 represent the specific experimental instrument used in this study: FEI Quanta 400 SEM.

This microscope is basically constituted by four parts:

- electrons source;
- vertical column through which electrons travel with electromagnetic lenses;
- electron detector; and
- vacuum chamber.

The imaging result is displayed at the computer interface.

Electron source produces electrons by thermionic heating, starting from three possible sources:

- Tungsten filament;
- solid state crystal of Cerium hexaboride (CeB_6) or Lanthanum hexaboride (LaB_6); and
- Field Emission Gun (FEG).

Electrons produced in electron source are accelerated with a voltage between 1 kV and 40 kV passing through a combination of lenses and apertures. Then a narrow beam is generated condensing electrons: the beam is finally used to extract images, analysing the echo coming from scanned surface.

In order to not influence the echo returning from surface, the electron microscope is designed to operate in vacuum. Hence the chamber must be evacuated before images can be acquired.

A schematic functioning is described in figure 27.

The position of electron beam is controlled by the scan coils above objective lens, which regulate the surface scanning phase.

The interaction of electron beam with sample surface produces backscattered electrons. To generate images, these secondary electrons are collected by one or more detectors and resulting signal is transformed by the software in a displayable picture. Each pixel of these acquired images represents the synchronized position of electrons beam on the sample, thus images can be considered as maps describing the distribution of signal intensity coming from scattered electrons.

SEM permits high magnifications up to 20000×, for this study images at 1000× were acquired. The examined cores were fixed on the plate in SEM vacuum chamber with carbon tape. In order to obtain a good view of lateral surface, the samples were positioned at a distance of 14 mm from the beam output and inclined with an angle of 40°.

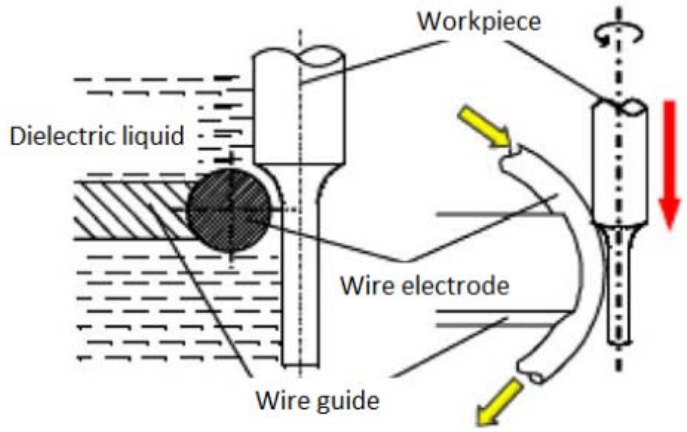

Figure 15. WEDG technology.

Figure 16. EDM processing.

Figure 17. Kugler Micromaster 5X.

Table 4. Definition of milling parameters.

Parameter	Definition	Unit
n	Rotation per minute	rpm
D_{cap}	Cutting diameter at actual D.O.F.	mm
f_z	Feed per tooth	mm
Z_n	Total number of teeth in cutter	-
Z_c	Number of effective teeth	-
v_f	Table feed	mm/min
f_n	Feed per rev	mm
a_p	Depth of cut (D.O.C.)	mm
a_e	Radial depth of cut (D.O.C.)	mm
v_c	Cutting speed	m/min

Figure 18. Micro milling processing.

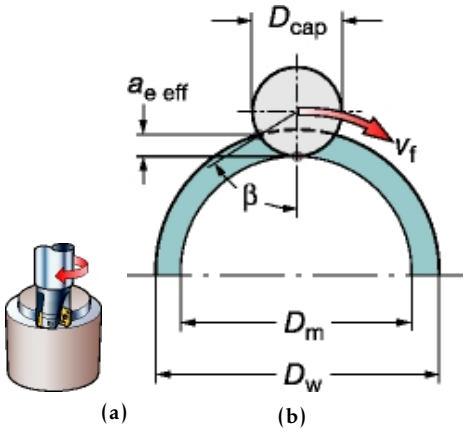

Figure 19. Description of milling process and parameters.

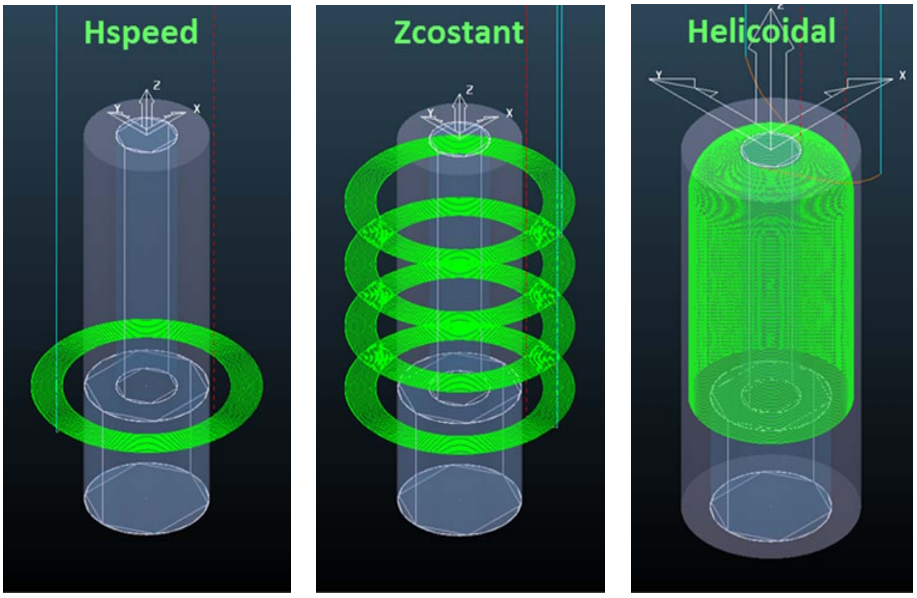

(a) *High speed* **(b)** *Z-constant* **(c)** *Helicoidal*

Figure 20. Different milling process approaches.

Table 5. Milling parameters for different approaches.

Strategy	Tool	D_{cap} mm	Z_c	n rpm	f_z mm	v_c m/min	v_f mm/min	a_p mm
High speed	BN	0.7	2	27 500	0.003	60	165	0.5
Z-constant	BN	0.7	2	27 500	0.003	60	165	
Helicoidal	BN	0.7	2	27 500	0.003	60	165	0.01

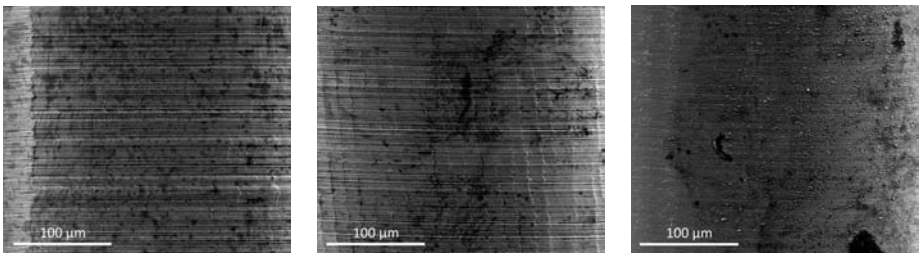

(a) *High speed.* **(b)** *Z-constant.* **(c)** *Helicoidal.*

Figure 21. SEM characterization of different milling approaches at 1000× magnification.

Table 6. Milling parameters evaluated to obtain the best result.

Test	Tool	D_{cap} mm	Z_c	n rpm	f_z mm	v_c m/min	v_f mm/min	a_p mm	time min
1	BN	0.7	2	20 000	0.001	44	40	0.01	15
2	BN	0.7	2	27 284	0.001	60	55	0.01	12
3	BN	0.7	2	50 000	0.001	110	100	0.01	6

Figure 22. Cores: the first from the left is uncoated, the second is coated with DLC-1, the third is coated with CrTiNbN, and the fourth is coated with DLC-2.

Table 9. Coatings properties.

Properties	Test method	DLC-1	DLC-2	CrTiNbN
Typology		ML grad.	ML grad.	Bilayer
Thickness (µm)	UNI 1071-2	2.0 ± 0.5	2.0 ± 0.5	3.0 ± 0.5
Adhesion (N)	UNI 1071-3	55 ± 4	55 ± 4	80 ± 5
Hardness (HV)	ISO 14577-1	2200 ± 300	2200 ± 300	2973 ± 263
Roughness (µm)	UNI 11255	0.10 ± 0.01	0.10 ± 0.01	0.17 ± 0.05
Tecnology		PACVD	PACVD	PVD
Adhesion layer		CrN	Cr	Cr

Table 10. Profiler properties.

Properties	20×	100×
Numerical aperture	0.45	0.90
Maximum slope (°)	21	51
Field of view (µm)	636×477	127×95
Spatial sampling (µm)	0.83	0.17
Optical resolution (µm)	0.31	0.15
Vertical resolution (nm)	<20	<2

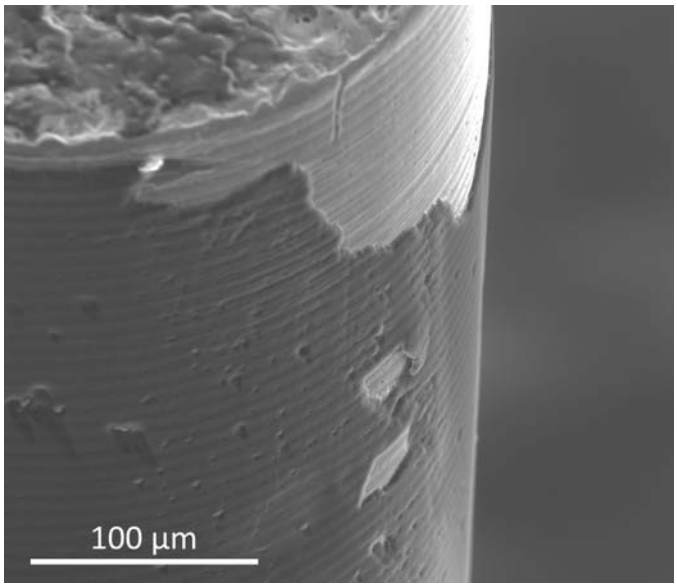

Figure 23. Damaged DLC coated surface.

Figure 24. Sensofar Plu neox.

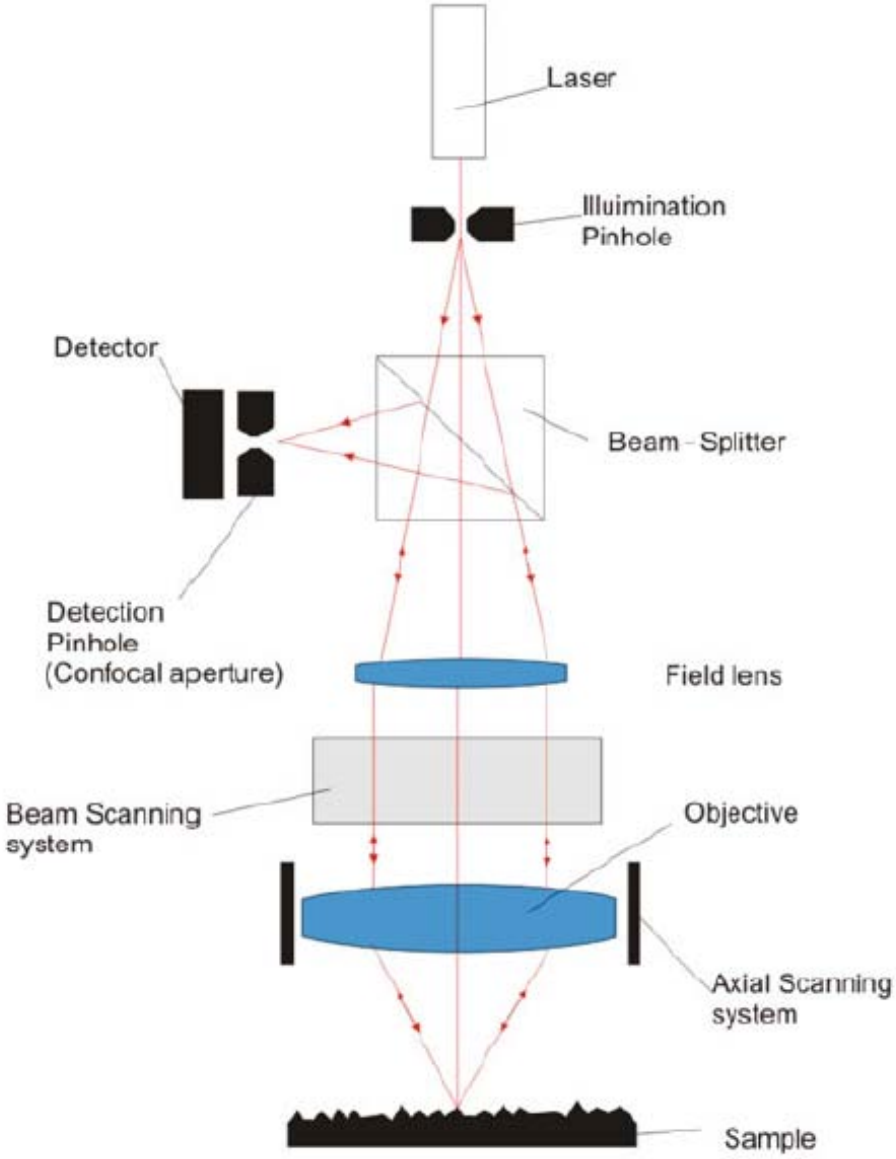

Figure 25. Scheme of basic setup of a laser scanning microscope with sample in focus position.

Figure 26. FEI Quanta 400 SEM.

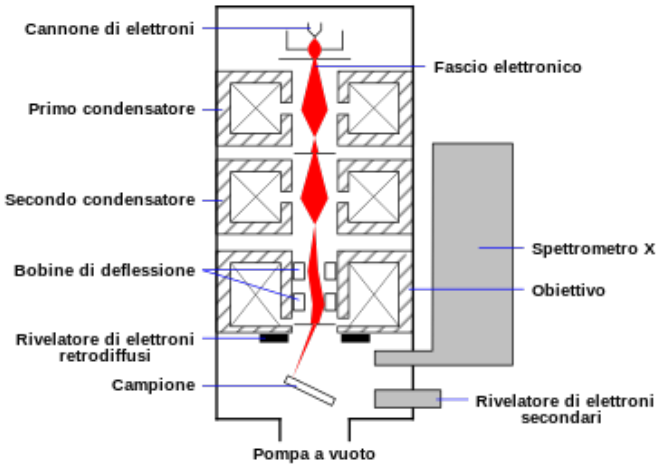

Figure 27. Scheme of basic setup of a scanning electron microscope.

Chapter 5

Micro injection moulding machine

Micro injection moulding is a process that must consider the applications of generated part. In fact, micro part should respond to strict requirements and tolerances. To do that a specific injection moulding machine has to be used: Micro Power 15 from Wittmann Battenfeld, represented in figure 28, was used in this study. Wittimann Battenfeld produces also machines for macro injection moulding, and the main differences between micro and macro machines lie in the proportion between mechanical parts: the lower limit of micro machine dimension are established by the strength of plunger and screw materials.

1. Characteristics of Micro Power 15

Principal characteristics of the Micro Power 15 are reported in the data sheet (table 11). Most important characteristics to notice are:

- maximum clamping force of 150 kN;
- maximum injection speed of 750 mm/s;
- diameter of plasticizing screw of 14 mm; and
- diameter of injection plunger of 5 mm.

All these values determine the range of part dimensions that can be moulded.

Injection system of Micro Power 15 is reported in figure 29 and is particular because plasticizing of polymer and injection in mould are separated. The screw plasticizes the material in an inclined path and the plunger acts horizontally. Usually for macro injection moulding machines these systems are coupled and both horizontal.

The material in the screw is melted by friction, the right injection moulding temperature is reached at the extreme section of the injection system thanks to

Figure 28. Wittmann Battenfeld - Micro Power 15.

Table 11. Wittmann Battenfeld - Micro Power 15 technical data sheet.

Properties	Unit	Value
Clamping unit		
Clamping force	kN	150
Opening stroke | Opening force	mm | kN	100 | 15
Ejector stroke | Ejector force	mm | kN	40 | 5
Injection unit		
Dosing screw diameter	mm	14
Dosing screw stroke	mm	26
Screw L/D ratio		20
Injection plunger diameter	mm	8
Specific injection pressure	bar	2500
Max. screw speed	min^{-1}	200
Max. plasticizing rate	g/s	1.7
Max. screw torque	N m	90
Nozzle stroke b | Contact force	mm | kN	230 | 40
Injection speed	mm/s	750
Injection rate into air	cm^3/s	38
Barrel heating power, nozzle inc.	kW	2.45
Drive		
Electrical power supply	kV A	9

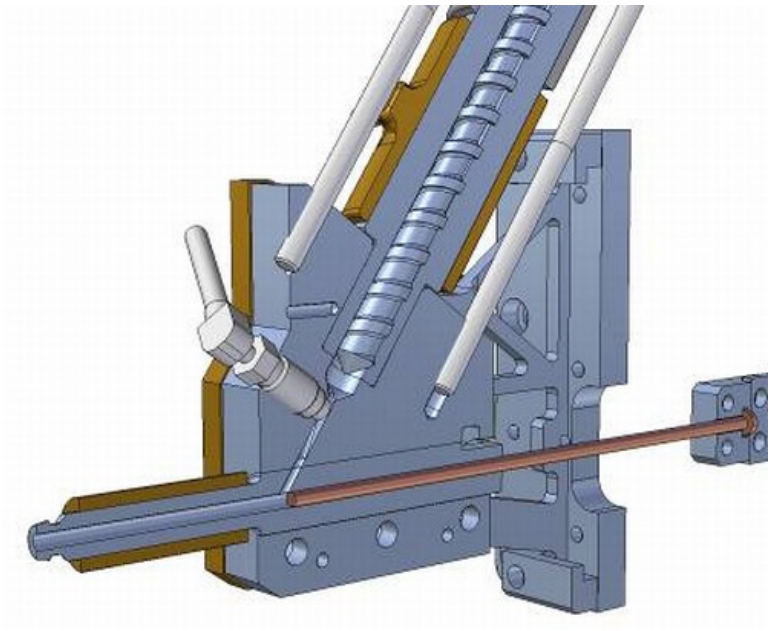

Figure 29. Injection system of Wittmann Battenfeld – Micro Power 15.

an internal heating circuit. Also the mould can be heated or cooled; to do that, heating and cooling circuits are located both in moving and fixed part of the mould. Figure 30 describes the position of these circuits: the right mould temperature is maintained with heated water in a hexagonal circuit) and electric resistances (horizontal bars). A transversal thermocouple measures mould temperature and interrupt heating process if temperature exceeds the selected value.

2. Demoulding force measurement and ejection system

In order to demould processed part four ejectors are used. In the centre of the mould there is a 5 mm ejector, and three 2 mm ejectors are located behind the cavity in the configuration that is shown in figure 31.

These three smaller ejection pins are longer than the fourth and are all connected with a plate. A plunger push the plate and ejection pins are moved contemporaneously. This configuration allows the part to be completely ejected by the smaller pins and in this way the ejection force measurement is not affected by larger ejector influence.

2.1. Acquisition sensor and software. The force variations during demoulding phase are measured by a KISTLER 9223A piezoelectric force transducer (figure 32), which has a measuring range of 2500 N. The sensor is located behind the ejection unit and moves together with the three ejection rods, in figure 31 this sensor is green coloured.

During the ejection stage the sensor is mechanical loaded and produces a piezoelectric charge signal, which is converted in an output voltage using a KISTLER

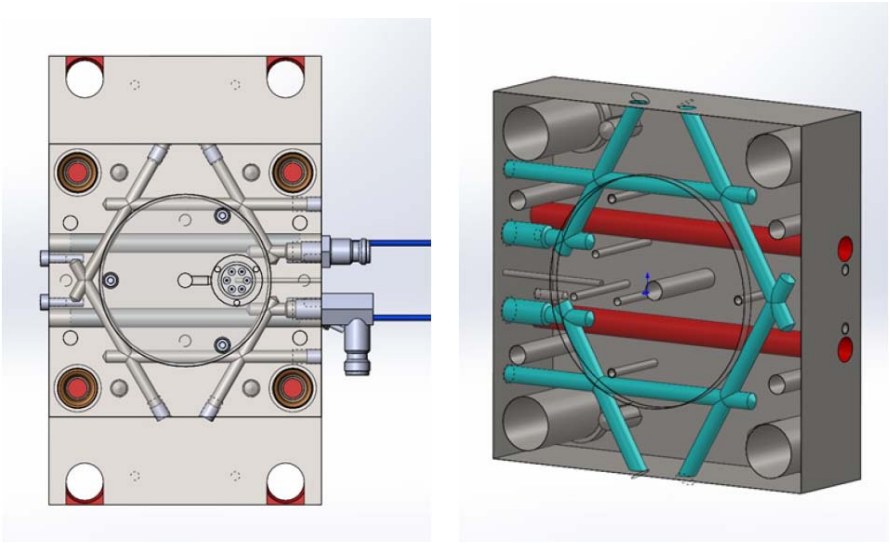

Figure 30. Heating and cooling systems in mobile mould part.

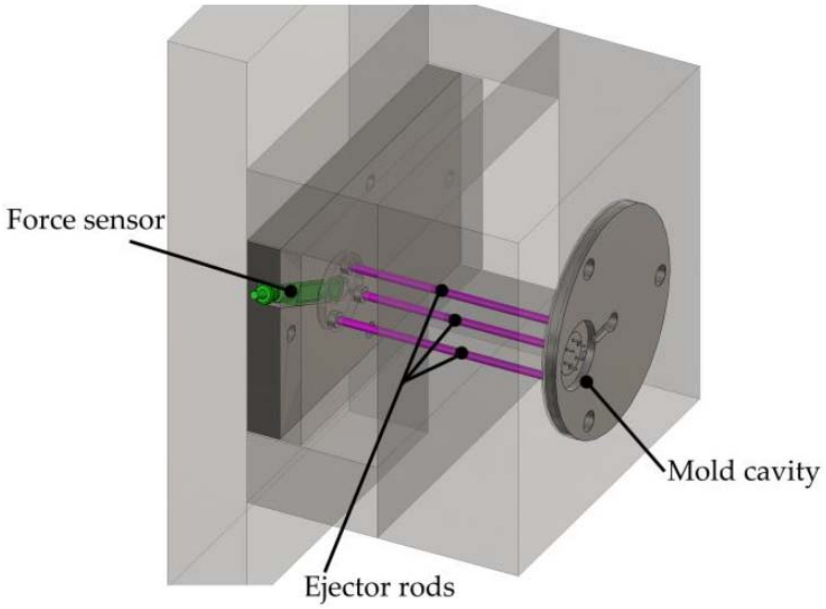

Figure 31. Ejection system and positioning of acquisition sensor.

Type 5039A charge amplifier. The transduced signal is then acquired by a National Instrument NI9205 16 bit analog input module. Then the sensor output signal

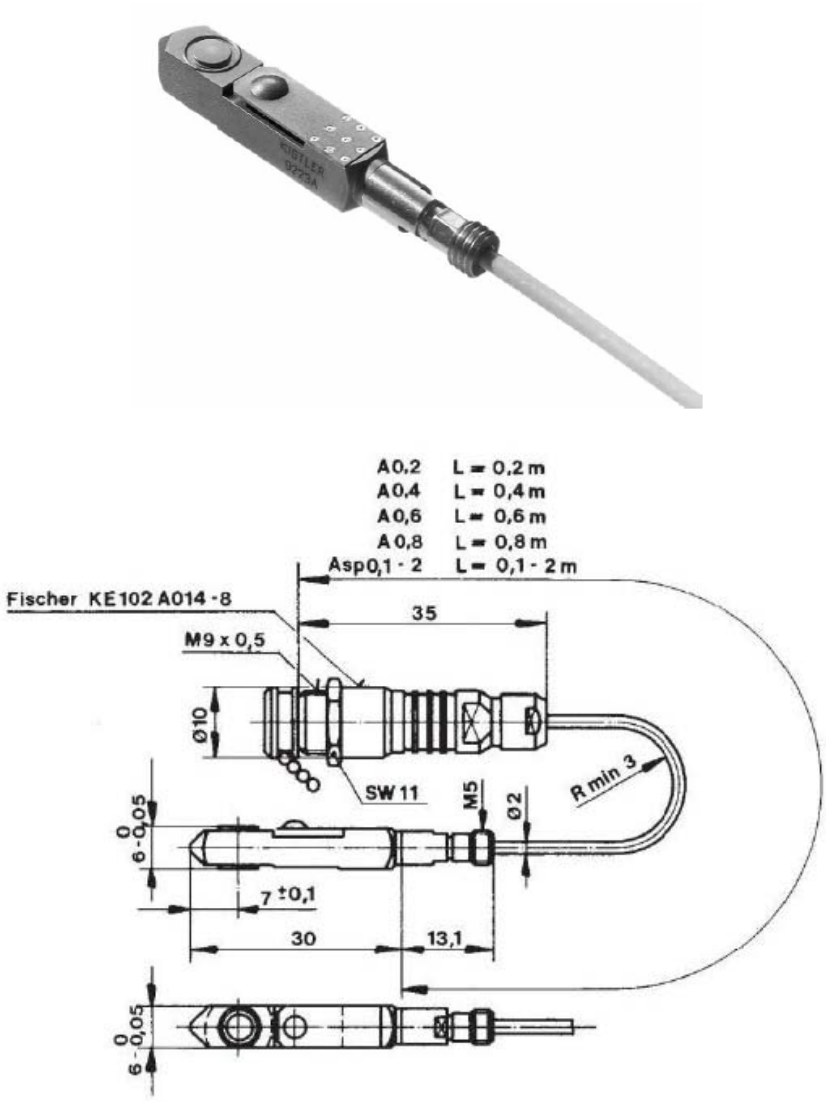

Figure 32. Acquisition sensor KISTLER 9223A.

is downloaded onto a PC by a National Instrument NI cDAQ-9172 data acquisition unit. Measured values are analysed with National Instrument LabVIEW 2013® software. In order to avoid any data loss the following parameters were set:

- force offset was left at null value;
- number of samples equal to 10;
- acquisition frequency of 60 kHz; and
- time steps between samples of 0.2 ms.

Part 3

Ejection forces analysis

Chapter 6

Surface characterization

First of all fabricated cores were analysed in their regularity and homogeneity by using x-ray computed tomography (CT, Nikon Metrology, MCT 225). Diameter variations were observed to be smaller than 3 µm, while deviations from cylindrical shape were found to be minor than 10 µm.

With the purpose of surface characterization of coated and uncoated cores, both a qualitative and a quantitative analysis were provided. The SEM allows detailed magnified images for a qualitative characterization, on the other hand quantitative results for surface characterization were obtained with profiler.

Images generated by SEM at 1000× are reported in figure 33 for a representative core of each set; morphology and continuity of coated surfaces were checked. Uncoated core (figure 33a) presents a very regular surface pattern, that is given from the micro milling process. Both DLC coatings are realized by PACVD technology: this method permits to obtain a smooth finished surface even if some defects affecting the coated surface can be seen in figures 33b and 33c. Whereas the PVD technology provides the CrTiNbN coating returning a wrinkly surface covered with microscopic agglomerations (figure 33d).

Both types of coating modify the core topography and it is interesting to notice that the different technologies used to coat the cores, influence the resulting superficial roughness, affecting the quality of the interface between injected material and mould surface. This fact could affect negatively the estimation of demoulding forces, because the adhesion effect could increase, due to superficial defects: superficial agglomerates act like undercuts during ejection phase and the mechanical interlocking between polymer and mould cores grows.

1. Roughness evaluation

In order to evaluate the superficial texture of cores, the topography of each core was analysed using the 3D optical profiler in confocal mode with a 20× objective.

For each core, four projected areas of 2.0 mm × 0.1 mm regularly distributed on the lateral surface were acquired, then three profiles each were analysed.

Using MountainsMap® software, roughness parameters were estimated applying a 0.08 mm Gaussian filter, then for each cores set the average value and the standard deviation were calculated. The software allows different analyses, for example figure 34 shows the main direction in which roughness values were estimated. This polar spectrum permits to observe that a preferential direction is almost perpendicular to the scanning way, and that is due to the milling process.

The profiler returns also a schematic image of surface topography, an example is reported in figure 35: different colours give a qualitative idea of the roughness distribution on the analysed surface.

The raw acquisition requires a series of filtering operations targeted to clean the measure from errors linked to shape deformations.

(1) Chose a restricted area in the centre of the acquisition, this avoids to analyse boundaries areas.

(2) Filter the image to remove cylindrical remaining shape.

(3) Filter again data with a 0.08 mm Gaussian filter.

An example of filtered result is figure 36 in which a roughness profile estimated in the considered restricted area can be observed.

According to ISO-25178, surface roughness parameters were estimated for each set: the results are available in table 12 and also in the first part of the relative plot (plot 6). The main result reflects the presence of the superficial coatings, in fact Sa average values, in case of coated core, are 62% higher than uncoated one. The same effect can be appreciated comparing Sz average values of coated cores with the reference value of uncoated case: DLC-1, DLC-2 and CrTiNbN present 26%, 38% and 47% of increase respectively.

Referring to ISO-15178, the Abbott-Firestone curves were evaluated. This curve provides informations about hills and valleys generated by the material deposition; these anomalies are important in the study of replication behaviour during the injection moulding process. These parameters are reported in table 13 and in the second part of the plot (plot 6). The Spk parameter describes the presence of peaks: the higher it is, the more it increases the friction between the mould and the part during demoulding phase. In this case the percentage increments are 54%, 45% and 73% respectively for DLC-1, DLC-2 and CrTiNbN. Moreover, the Svk value indicates the relevance of void volumes distributed on the core surface. During injection process these voids are filled and undercuts are created: this causes an higher interaction at the interface during the ejection of the part. Also in this case the coated cores present an higher Svk value in comparison with uncoated cores: increments are 25%, 19% and 31% for DLC-1, DLC-2 and CrTiNbN.

In a similar way, also profile roughness parameters were estimated according to ISO-4278; results can be examined numerically from table 14 and they are plotted in plot 7 for a visual explanation. As like as in the analysis of surface roughness parameters, also for profile roughness parameters the increments of Ra compared to uncoated case are 157%, 114% and 86% respectively for DLC-1, DLC-2 and

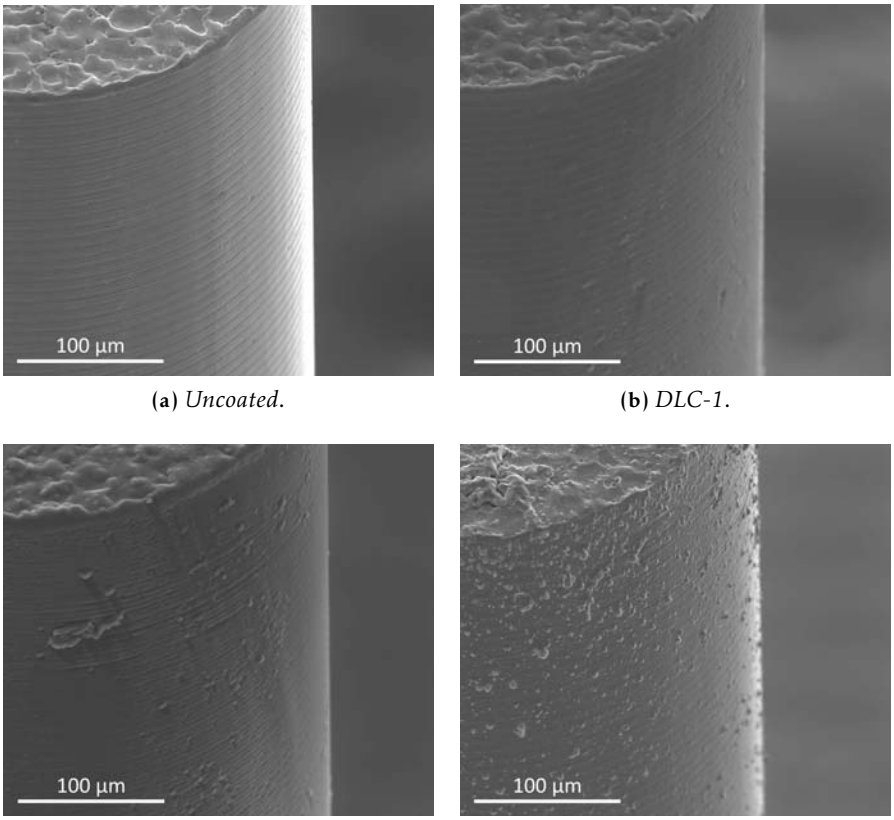

(a) *Uncoated*. **(b)** *DLC-1*.

(c) *DLC-2*. **(d)** *CrTiNbN*.

Figure 33. SEM characterization of micro cores at 1000× magnification.

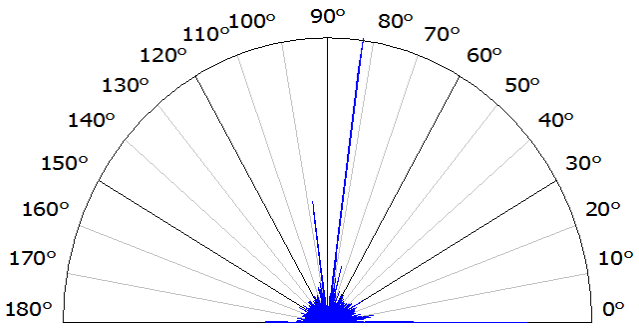

Figure 34. Example of roughness values distribution: polar spectrum.

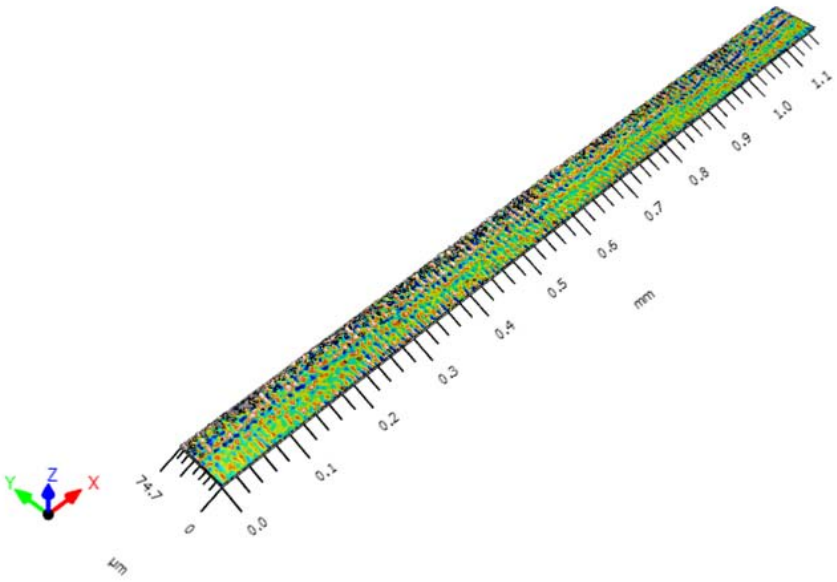

Figure 35. Example of surface topography characterized with profiler.

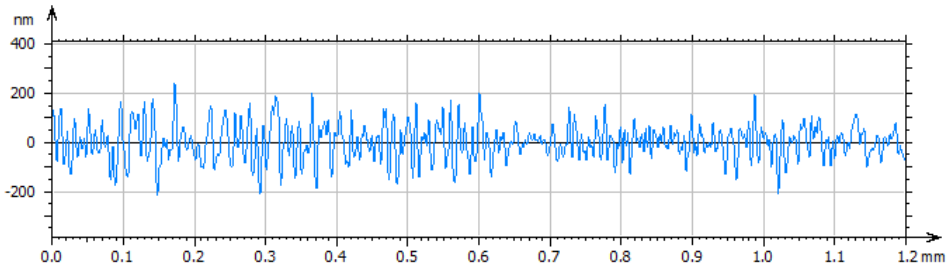

Figure 36. Example of profile roughness estimated in a restricted area of the core surface.

Table 12. Average values (A.V.) and standard deviation (S.D.) of surface roughness parameters evaluated according to ISO-25178.

ISO-25178								
Coating	Sa (µm)		Sp (µm)		Sv (µm)		Sz (µm)	
	A.V.	S.D.	A.V.	S.D.	A.V.	S.D.	A.V.	D.S.
Uncoated	0.08	0.01	1.26	0.83	1.30	0.69	2.57	1.51
DLC-1	0.13	0.02	3.46	1.33	2.01	0.42	5.48	1.44
DLC-2	0.12	0.01	3.16	1.40	2.13	0.22	5.28	1.36
CrTiNbN	0.13	0.03	2.03	1.23	1.74	0.33	3.77	1.50

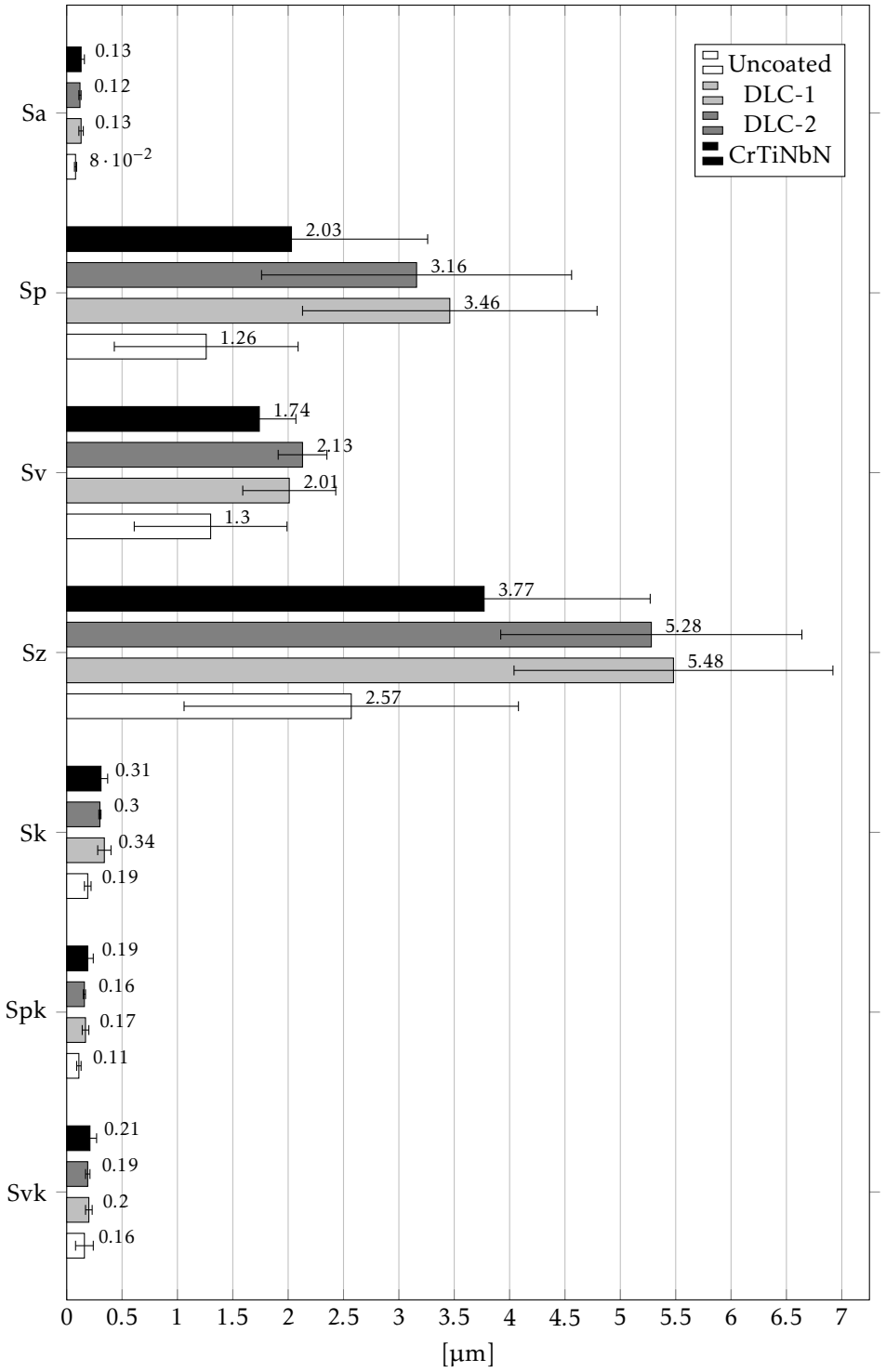

Plot 6. Profile roughness parameters evaluated according to ISO-4287 and ISO-13565-2.

CrTiNbN coating. Furthermore Rz value increases respectively of 156%,127% and 102% for DLC-1, DLC-2 and CrTiNbN.

The evaluation of all these parameters (referred both to surface and profile) confirms that superficial coatings affect the regular surface texture, typical of micro milling process, introducing some defects that cannot be neglected.

Referring this time to ISO-13565-2 the Abbott-Firestone curves were evaluated. Rpk corresponds to Spk, but it refers to the profile analysis: also in this case the coatings provide increments that are 1110%, 167% and 200% respectively for DLC-1, DLC-2 and CrTiNbN. In addition, Rvk is referable to the superficial parameter Svk, and like the previous cases, the values in comparison with uncoated cores increase: 193%, 164% and 100% for DLC-1, DLC-2 and CrTiNbN.

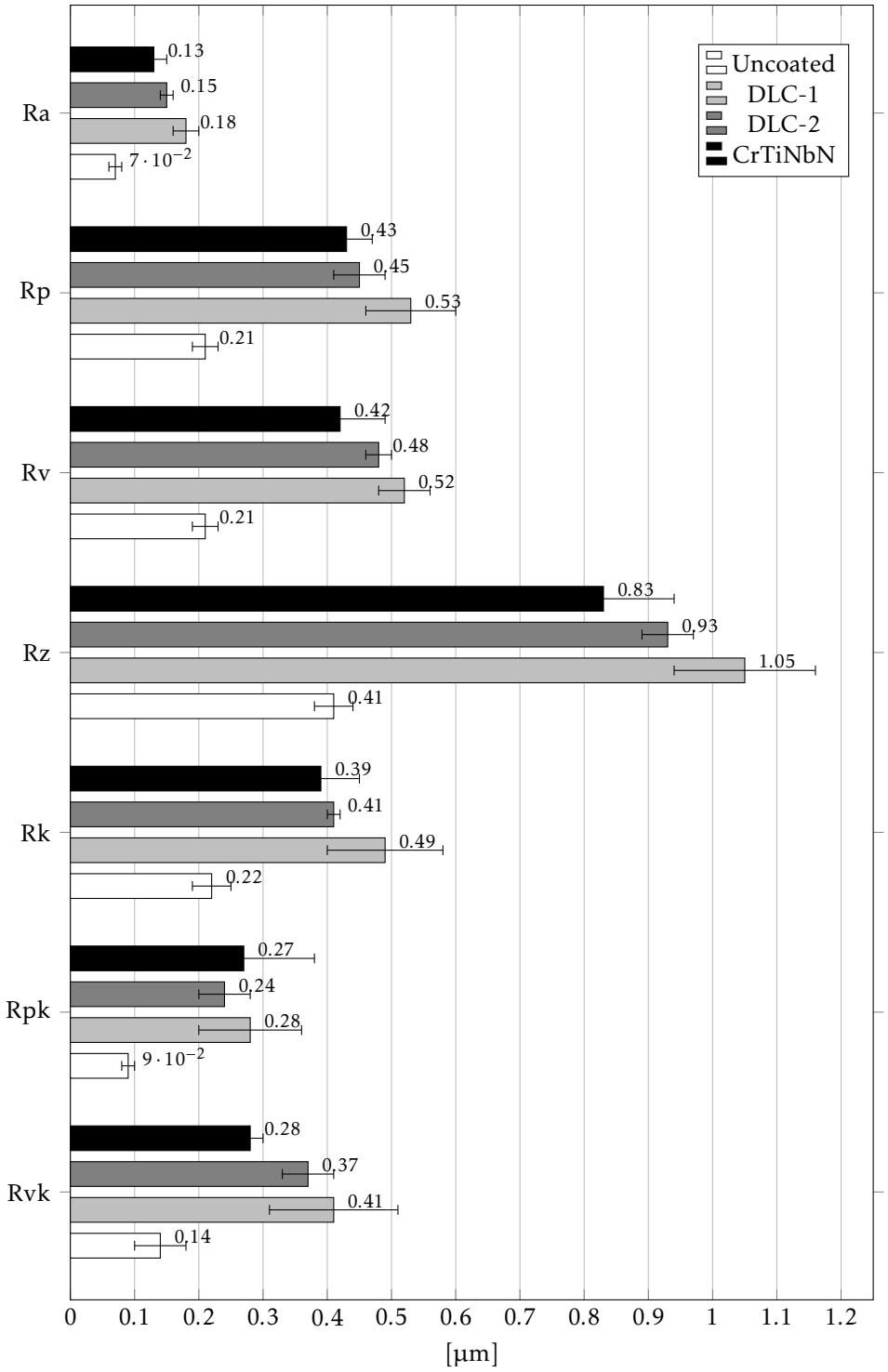

Plot 7. Profile roughness parameters evaluated according to ISO-4287 and ISO-13565-2.

Table 13. Average values (A.V.) and standard deviation (S.D.) of surface roughness parameters evaluated according to ISO-15178.

ISO-15178						
Coating	Sk (µm)		Spk (µm)		Svk (µm)	
	A.V.	S.D.	A.V.	S.D.	A.V.	S.D.
Uncoated	0.19	0.03	0.11	0.02	0.16	0.08
DLC-1	0.34	0.06	0.17	0.03	0.20	0.03
DLC-2	0.30	0.01	0.16	0.01	0.19	0.02
CrTiNbN	0.31	0.06	0.19	0.05	0.21	0.06

Table 14. Average values (A.V.) and standard deviation (S.D.) of profile roughness parameters evaluated according to ISO-4278.

ISO-4287								
Coating	Ra (µm)		Rp (µm)		Rv (µm)		Rz (µm)	
	A.V.	S.D.	A.V.	S.D.	A.V.	S.D.	A.V.	D.S.
Uncoated	0.07	0.01	0.21	0.02	0.21	0.02	0.41	0.03
DLC-1	0.18	0.02	0.53	0.07	0.52	0.04	1.05	0.11
DLC-2	0.15	0.01	0.45	0.04	0.48	0.02	0.93	0.04
CrTiNbN	0.13	0.02	0.43	0.04	0.42	0.07	0.83	0.11

Table 15. Average values (A.V.) and standard deviation (S.D.) of profile roughness parameters evaluated according to ISO-13565-2.

ISO-13565-2						
Coating	Rk (µm)		Rpk (µm)		Rvk (µm)	
	A.V.	S.D.	A.V.	S.D.	A.V.	S.D.
Uncoated	0.22	0.03	0.09	0.01	0.14	0.04
DLC-1	0.49	0.09	0.28	0.08	0.41	0.10
DLC-2	0.41	0.01	0.24	0.04	0.37	0.04
CrTiNbN	0.39	0.06	0.27	0.11	0.28	0.02

Chapter 7

Wettability

This study proposes the analysis of correlation between different surface coatings and ejection forces for various injected materials. Therefore wettability properties have an important role in estimation of interactions between coating material and polymer.

If a coating is well wettable, that means a major interaction coating-polymer and this leads to a better replication of surface topography of the mould. On the other hand a low wettable coating generates a chemical barrier between itself and the polymer and the injected material has difficulties in replication. Thus a good chemical affinity permits to obtain a better reproduced mould and ideally ah higher ejection force peak: these two effects must be balanced to obtain the best result in replication without increasing to much ejection costs.

The parameter to consider in order to evaluate wettability of materials is the contact angle at the interface between polymer drop and coated surface. A good wettability of an injected material is determined by a small contact angle, conversely a great angle means worse capability of wettability.

1. Wettability evaluation

Figure 37 shows the experimental results of wettability tests: drops of polymers were melted over coated surfaces. For different combinations of coated surface and melting polymer, the contact angle was evaluated.

In a qualitative way, an higher wettability can be noticed for PS, instead the worst wettability properties belong to PA.

In table 16 estimated values of contact angles for all the combinations are reported.

As qualitatively expected PS has the smallest average contact angles transversely for all the different coatings and PA the greatest, POM and COC have comparable resulting contact angles. This can be easily seen in plot 8.

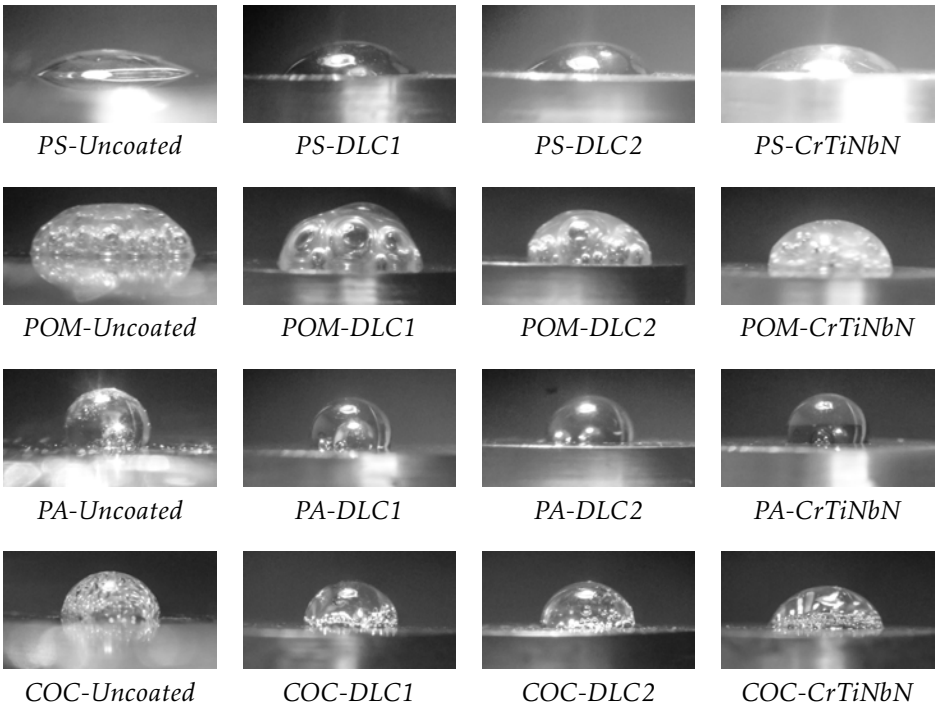

Figure 37. Wettability evaluation.

Influence of coating on wettability properties of each considered polymer is low, in fact form plot 9 derives that coatings have almost the same effect with all the polymers.

The wetting behaviour of melted polymers on coated surfaces is affected both by polymer and coating. However, the influence of the coating can be neglected in comparison with melted material nature.

The increment of contact angle changing material from PS to PA is on average of 96%, changing from PS to POM results on average of 64% and from PS to COC is 72%. Conversely contact angle increments from uncoated case to different coatings in the worst case of 16% (DLC-1 with PS).

Table 16. Average value (A.V.) and standard deviation (S.D.) of contact angle [°] for each material-coating combination.

Material	Uncoated		DLC-1		DLC-2		CrTiNbN	
	A.V.	S.D.	A.V.	S.D.	A.V.	S.D.	A.V.	S.D.
PS	44.52	1.35	51.21	1.77	42.63	1.85	46.73	1.93
POM	72.32	2.01	69.25	2.05	80.95	2.47	73.01	1.98
PA	93.51	0.73	96.01	1.41	90.02	0.57	82.21	1.13
COC	83.13	3.03	84.61	0.75	72.73	1.81	77.89	1.76

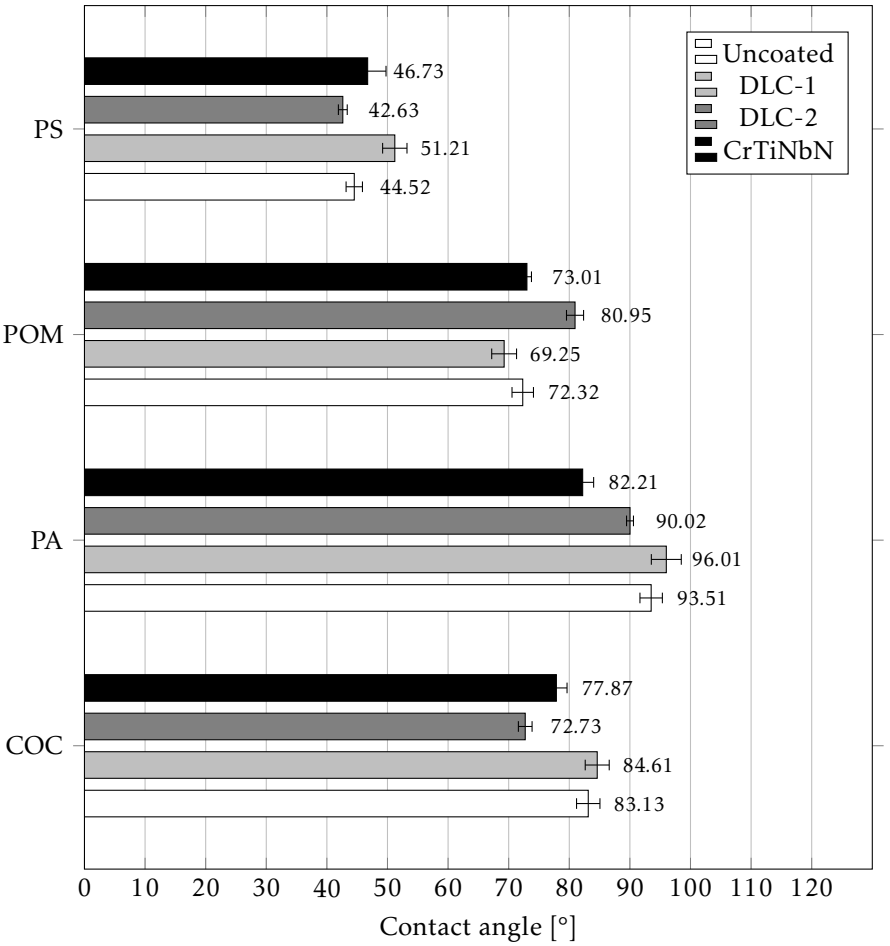

Plot 8. Plot of contact angles estimated through wettability analysis and evaluated for different material-coating combinations.

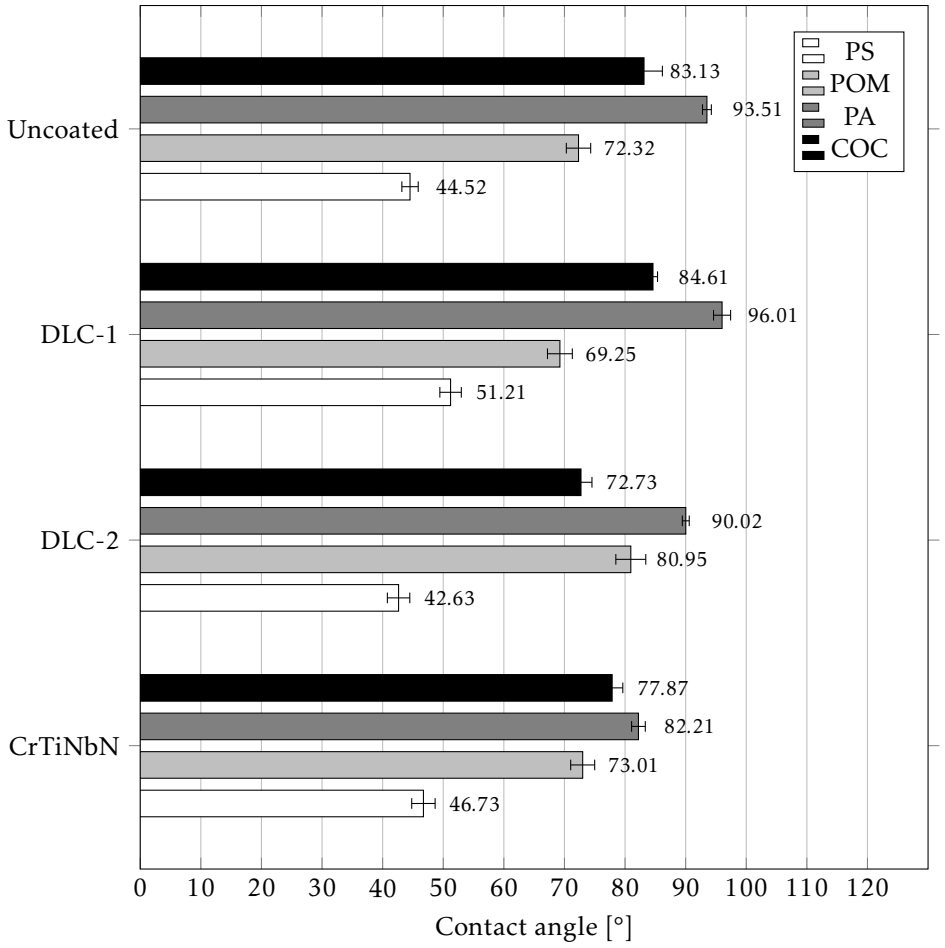

Plot 9. Plot of contact angles estimated through wettability analysis and evaluated for different material-coating combinations.

Chapter 8

Ejection forces measurement

The principal aim of the study was to observe and analyse the behaviour of different injected polymers at the variation of superficial mould coating.

To investigate the ejection forces a piezoelectric force transducer was used. The sensor collects force values in time and for each acquisition returns a plot like the one in plot 10. The demoulding force peak F_{peak} represents the maximum value of load that stresses the part during ejection phase. This peak was selected as reference variable for the analysis.

With the purpose to guarantee a stable injection moulding process, 50 moulding cycles were accomplished before the beginning of the acquisition trial. To have repeatable measures and to avoid systematic errors 30 acquisition every 5 cycles were collected. This procedure took place for each combination between injected material and coating.

Results for each combination were collected and elaborated to obtain an average peak force value with a corresponding standard deviation, as it is reported in table 17.

Plot 11 shows the incidence of the different injected polymers in relation with the same coating, and vice versa the effect of different coatings on the same material.

It can easily observed that COC is the polymer that presents the higher demoulding force peak at the varying of coatings. Furthermore, demoulding parts from uncoated moulds is less expensive in terms of ejection force required than from coated ones.

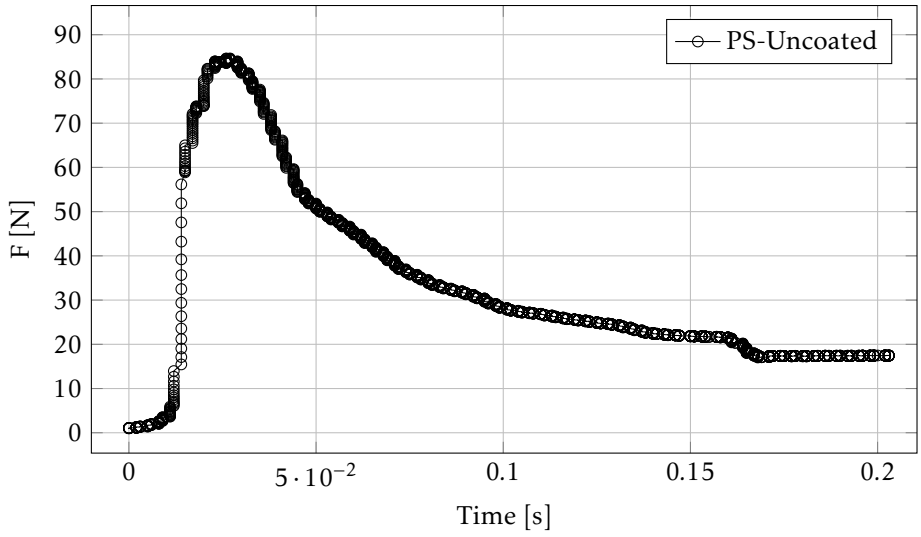

Plot 10. Example of ejection force monitored by the sensor: the maximum value is F_{peak}.

Table 17. Average value (A.V.) and standard deviation (S.D.) of ejection force peak [N] for each material-coating combination.

Material	Uncoated		DLC-1		DLC-2		CrTiNbN	
	A.V.	S.D.	A.V.	S.D.	A.V.	S.D.	A.V.	S.D.
PS	84.62	0.35	105.61	0.38	111.25	1.10	103.44	0.90
POM	49.59	0.28	59.52	0.64	53.51	0.41	56.38	0.33
PA	62.54	3.31	60.91	1.65	61.06	2.67	65.71	2.37
COC	199.42	6.03	223.37	4.32	256.40	2.86	238.93	0.36

1. Material-coating interactions

Results can be analysed in two different ways: for the same material the influence of different coatings can be observed, or for the same coating the effect of various polymer can be tested. Plots 12 and 14 permit to compare respectively the behaviour of materials and coatings.

1.1. Force variation related to different materials. Plot 12 shows that the behaviour of each material is almost always the same when compared with different coatings: using POM, the friction during ejection phase in each considered case is minimized. Instead, if COC is injected, friction is maximum. Bringing POM as reference (in case of uncoated cores), the increments in demoulding force peak value are respectively 26% for PA, 71% for PS and 302% for COC.

The similar behaviour of each polymer in different coating conditions is due to its rheological and tribological properties. Viscosity is directly linked to the polymer replication power of the mould superficial topography: the more viscous

the material is, the worse the replication results. In fact, if viscosity is low, it is easy for the polymer to fill the voids on mould surface during pressurized injection phase. Consequently a interlocking at the interface between polymer and mould surface is produced, and the ejection force required to start the sliding of the solidified polymer in order to demould the part is higher.

Wettability is another parameter that influences the demoulding force. In section 1 was supposed that an low value of contact angle corresponds to a good replicability and consequently to an higher ejection force value. This results was confirmed for PS in comparison with PA; in fact PS presents an higher ejection force peak and a smaller contact angle compared to PA. On the contrary POM presents an lower ejection force peak but it has also a lower wettability. The last consideration is that COC and POM present almost the same behaviour during wettability tests but ejection force peak evaluated for POM is the lowest among the selected materials and the one for COC is the highest.

In order to estimate the behaviour of different materials during ejection phase, it is necessary to consider both wettability and viscosity at the same time. For example PS has a low viscosity and a low contact angle, so the ejection force peak is high; but COC presents a greater contact angle and a lower viscosity compared to PS and its F_{peak} is higher. As said, POM and COC have almost the same wetting behaviour but the first presents an higher viscosity value determining a lower ejection force peak.

In general tribological conditions at the interface between part and mould are affected both by the chemical adhesion due to the combination of materials and by the rheological properties of the melting polymer. Moreover the effects of these properties should be considered together interacting.

1.2. Force variation related to different coatings. The other way to interpret the data is to compare the behaviour of each injected polymer at the variation of coating.

Surface treatments can largely affect the resulting ejection force peak value, and looking at plot 14 different trends for the selected material can be noticed. In fact the chemical interaction between superficial coating and moulding material is the main responsible of different F_{peak} values for the same injected polymer.

Except PA, polymers present lower demoulding force in case of uncoated cores: in particular COC, which sees an increase of 12% for DLC-1, of 29% for DLC-2 and of 20% for CrTiNbN in comparison with uncoated case. Both COC and PS have a high affinity with DLC-2, which causes the force value to be higher than the case with DLC-2: this can be explained remembering that the adhesion layer of two DLC coatings was different (CrN for DLC-1 and Cr for DLC-2). Conversely POM and PA show a better affinity with DLC-1.

Another parameter that is interesting to consider is the superficial roughness: except for PA again, considering a certain material the higher demoulding forces were estimated when a coated core set was used. This means that an higher interface interaction due to mechanical interference and fiction between mould and part is a consequence of the agglomerations that characterize the coated surfaces.

Considering viscosity as a fundamental property of material and roughness characteristic of coating, their interaction can be analysed. The demoulding force increases when a combination of low viscosity material and cores with high surface roughness are used, because of the hard mechanical interlocking at the interface. On the other hand F_{peak} decreases when viscosity is high and surface is smooth.

2. Different parameters together interactions

At least in order to estimate the behaviour of different polymer during ejection phase, four parameters should be taken in consideration: roughness, wettability, viscosity and coating.

2.1. Trends definition. Plot 15 represent the correlation between wettability properties (linked to contact angle) and different coating, acting on ejection force peak. This plot indicates that higher values of contact angles correspond to a lower demoulding force, with exception of materials characterized by the combination of very low viscosity and high contact angle, as COC.

Regression lines show a almost linear behaviour of each material at the varying of surface coating.

The last plot (figure 38) report the fitting surface of experimental data correlated each other by roughness (Sz) and viscosity (η).

The main aim of this last two plots is the possibility of making prevision about the behaviour of different material, if properties of injected material and of the mould are known. In order to improve this representation methods and to fit better the real behaviour of moulding materials more experimental data are needed.

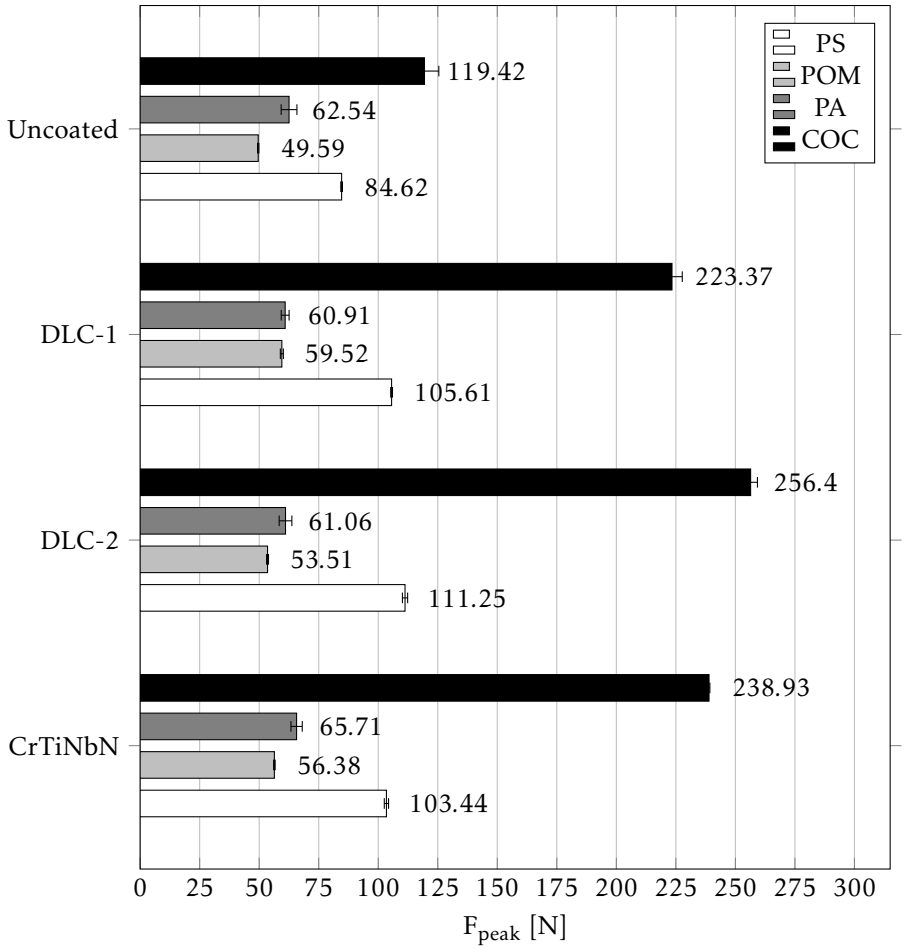

Plot 11. Plot of ejection force peaks evaluated for different material-coating combinations.

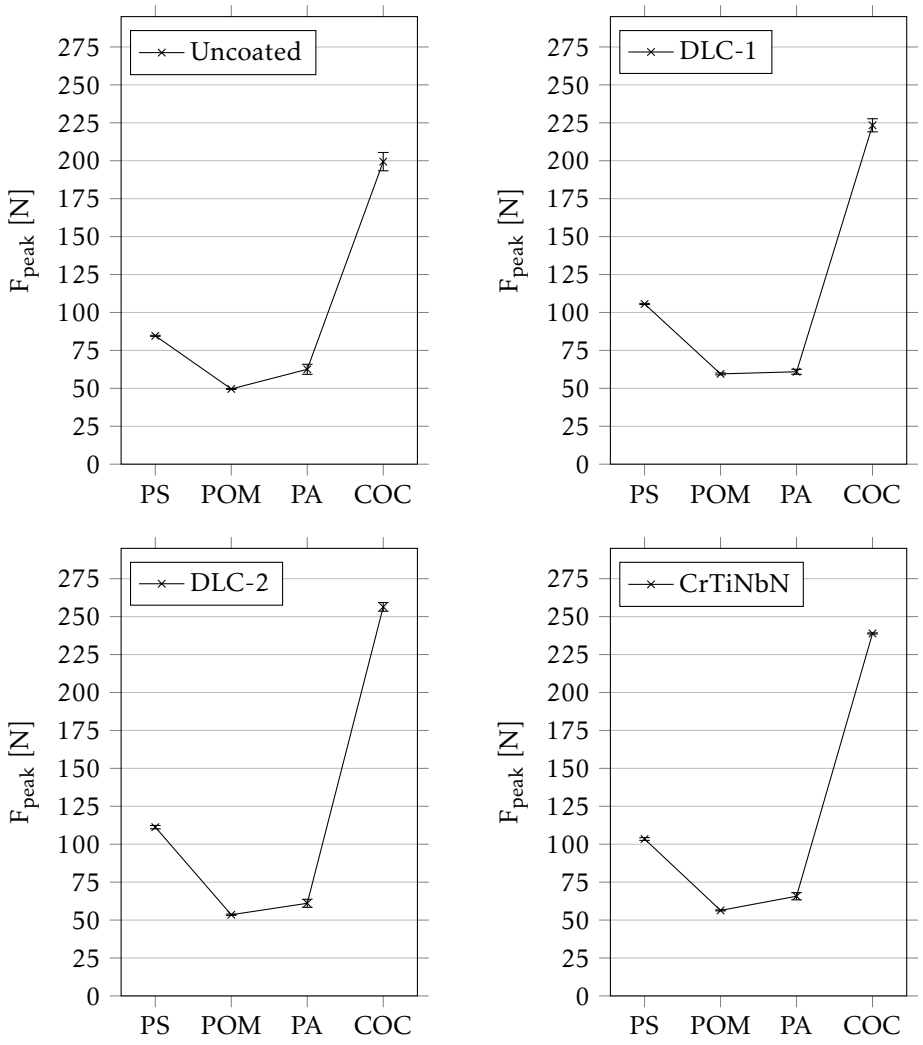

Plot 12. Variation of ejection force peak related to different materials.

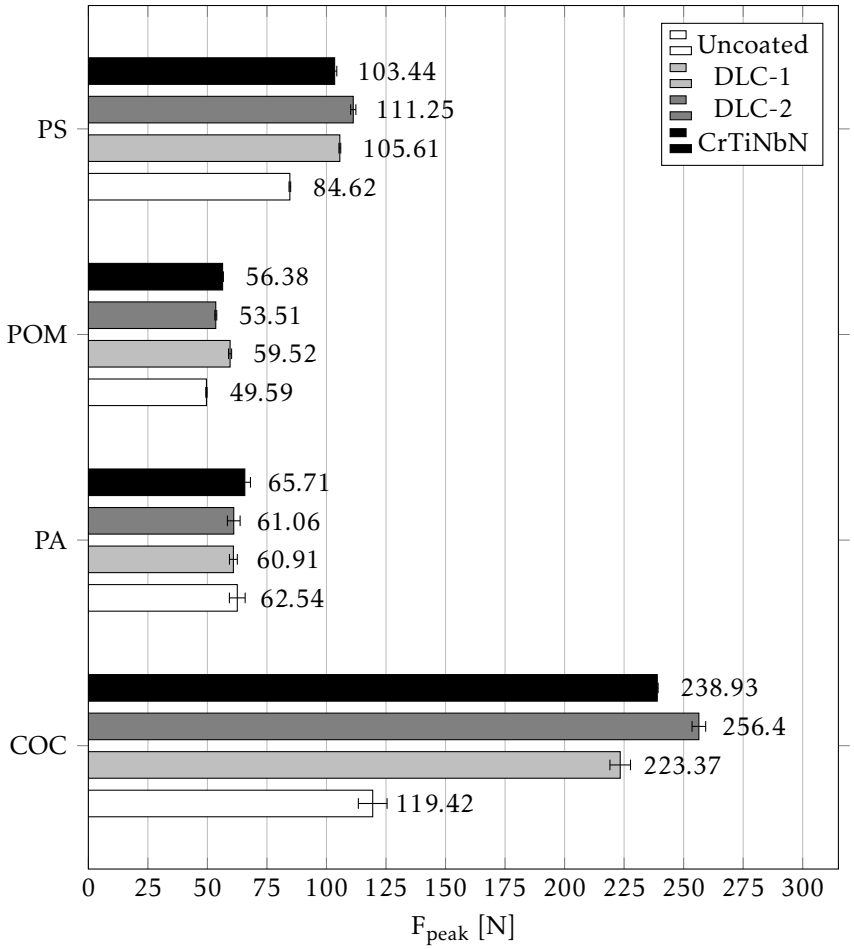

Plot 13. Plot of ejection force peaks evaluated for different material-coating combinations.

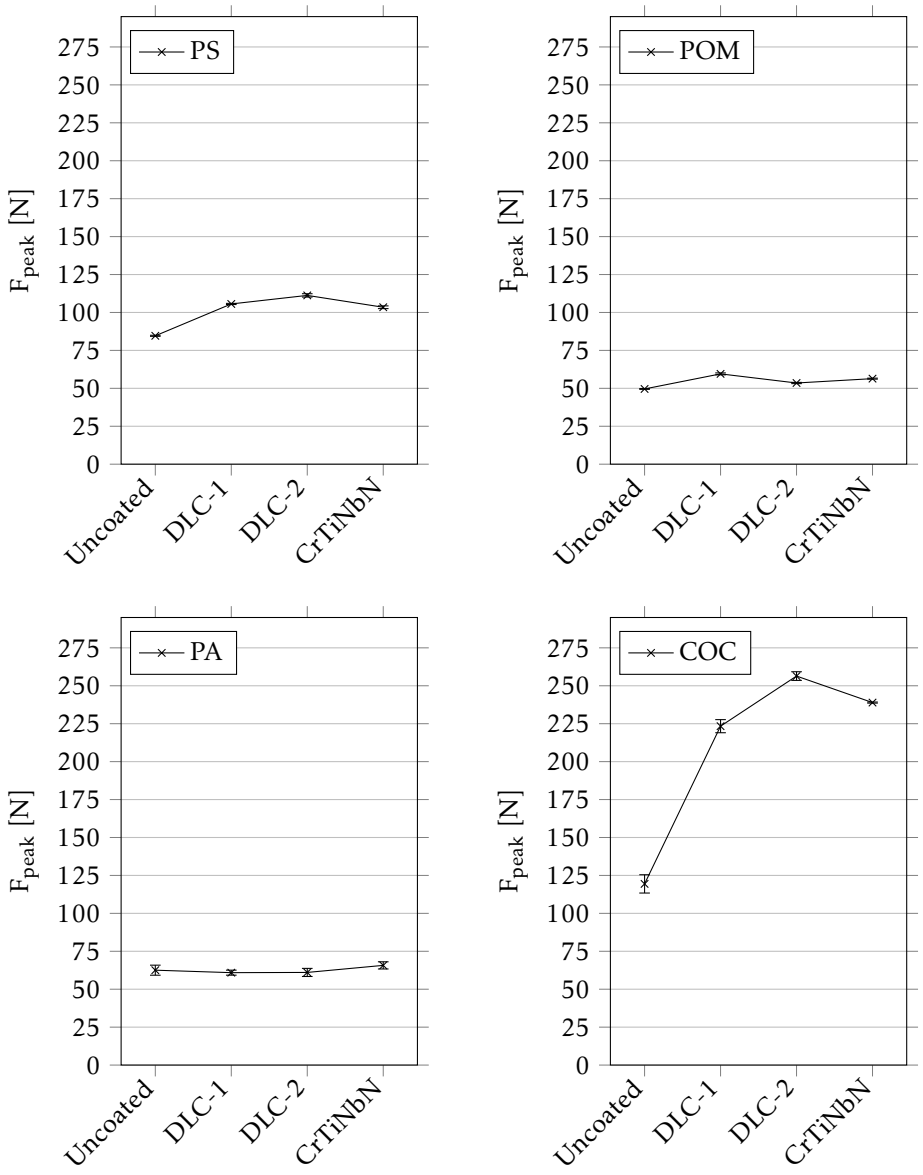

Plot 14. Variation of ejection force peak related to different coatings.

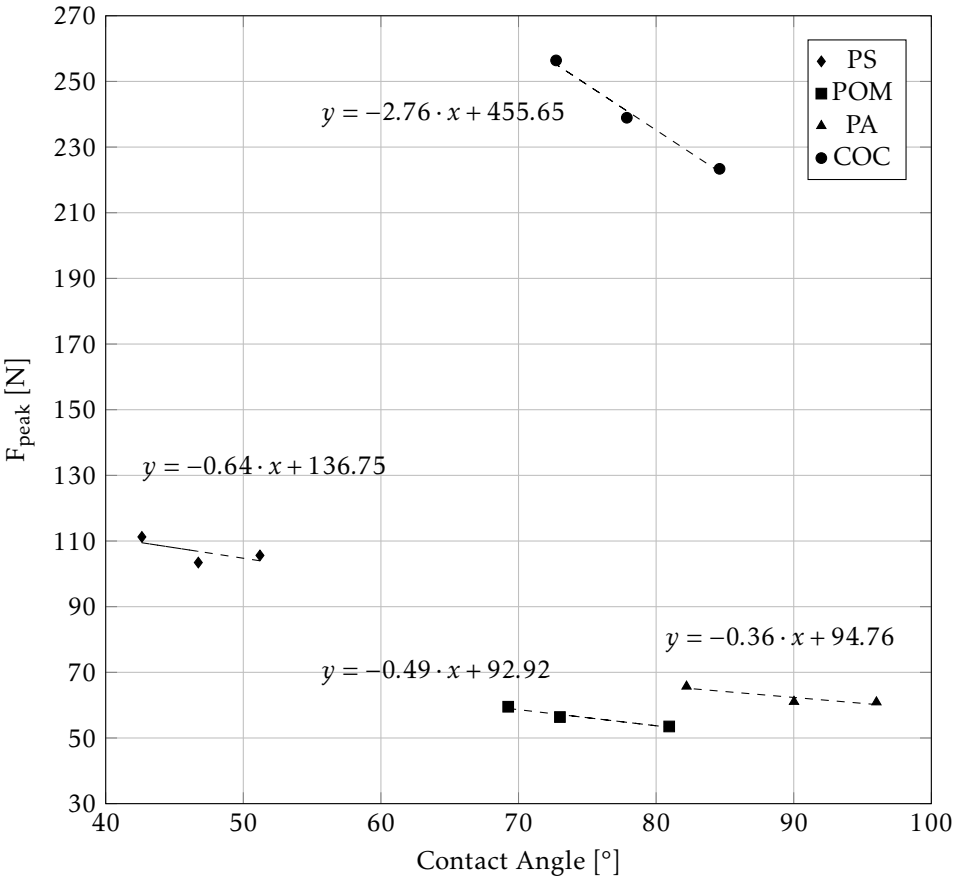

Plot 15. Plot of ejection force peak for each material, related to contact angles of different coatings. The regression line fit data for each set of coatings.

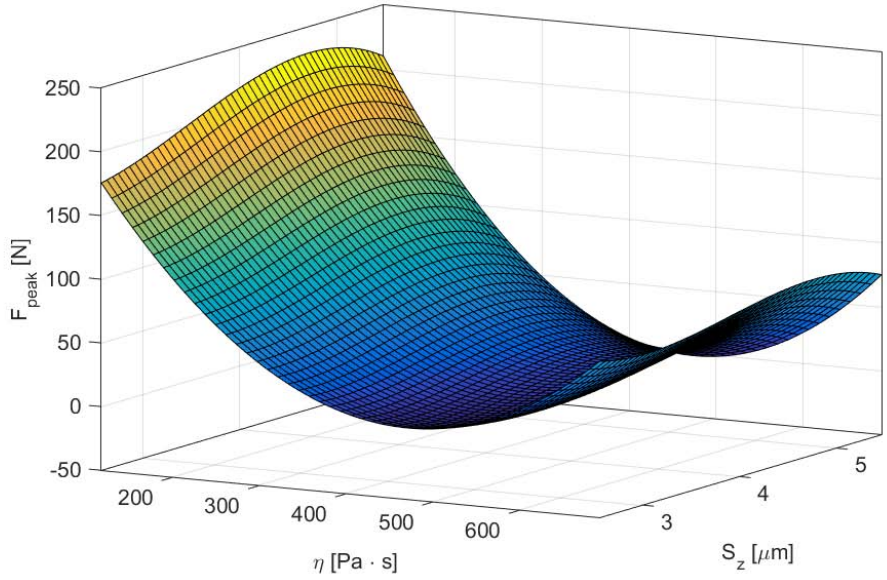

Figure 38. Surface plot representing the interacting effect on ejection force peak of polymer viscosity and surface roughness.

Part 4

Conclusions

Chapter 9

Conclusions

The aim of this study was to analyse the effects of various mould coatings on ejection force in micro injection moulding, for different thermoplastic polymers. Four polymers were selected (PS, POM, PA6, COC) and three coatings were considered (two types of DLC with different adhesion layer and a CrTiNbN coating).

A mould cavity was designed to present interchangeable cores, that were manufactured by micro milling and successively coated. An entire set was left uncoated in order to compare different behaviours.

Cores were characterized in topography and geometry with a x-ray computed tomography, a profiler and a SEM. Than roughness parameters were estimated using MountainsMap® software, in order to isolate the effect of interface phenomena.

Qualitative observation of coated surfaces demonstrated that coatings changed superficial topography with agglomerates and defects due to the coating strategies involved. Different values of surface roughness were obtained and this affected negatively demoulding phase.

Wettability properties of polymers were investigate evaluating for each combination the contact angle between polymer and coated surface. Viscosity was numerically analysed applying William-Landel-Ferry model.

Ejection forces for each considered case were acquired by a piezoelectric force transducer. Resulting maximum value for each polymer-coating combination was registered. Elaborated results showed that demoulding force peak is affected both by polymer and coating material.

Wettability data, viscosity properties, roughness estimation and ejection force values were combined in different ways in order to discover main interactions between them.

Main conclusions are following.

(1) In case of micro parts coated cores affect ejection forces worse than uncoated ones, because of the presence of agglomerates that produce a wrinkly and irregular contact surface.

(2) Polymers with higher wettability properties require higher ejection forces, because of the best replication of surface defects.

(3) More viscous polymer affects negatively demoulding phase, because of the best ability in filling surface voids.

(4) The same polymer responds diversely to different coatings, because of different chemical affinity.

Even if coating properties are the same for various polymers, injected materials with different combinations of wettability properties and viscosity present different behaviours in demoulding phase. Therefore, prediction of ejection force value must take in consideration all interactions between rheological, tribological and chemical parameters.

In conclusion the most important plot was reported in section 2.1: a linear regression was observed between contact angle value and ejection force peak.

1. Future developments

Future studies in the same ambit could be researches of behaviour evaluating for the same polymers, but with different coatings. In this way more experimental data could fill the plot that relates ejection forces to contact angle. If a linear law could be defined, behaviour of different materials with any coating could be predict by a simple wettability test.

An other development of this study could be the comparison of micro and macro cores, using the same materials and coatings.

Part 5

Appendix

Appendix A

Datasheets of polymers

POLYSTYRENE CRYSTAL 1540

Refining & Chemicals
Polymers

Technical Data Sheet
Easy Flow crystal Polystyrene
Manufactured in Europe

Description

POLYSTYRENE CRYSTAL 1540 is an easy flowing crystal polystyrene designed for extrusion or injection applications. In extrusion, it allows to increase extruder output and thermoforming cycle times when mixed with a high impact polystyrene such as POLYSTYRENE IMPACT 7240. Having high gloss, it is particularly suitable for glossy-layer co-extrusion. In injection moulding, POLYSTYRENE CRYSTAL 1540 with this low viscosity at high shear rate has a good injectability and combines an excellent fluidity with a higher softening point.

Applications

Dairy sheet, cups (dilution with impact polystyrene)

Injection: Boxes, office equipment - e.g. filing trays, CD boxes, pen bodies, internal fridge parts, toys, cups.

Properties

Rheological	Method	Unit	Value
Melt flow index (200°C-5kg)	ISO 1133 H	g/10mn	12
Thermal			
Vicat softening point 10N (T° increase = 50°C/h)	ISO 306A50	°C	91
Vicat softening point 50N (T° increase = 50°C/h)	ISO 306B50	°C	86
HDT unannealed under 1.8 MPa	ISO 75-2A	°C	73
HDT annealed under 1.8 MPa	ISO 75-2A	°C	83
Coefficient of linear thermal expansion		mm/°C	7.10 E-5
Mechanical			
Unnotched Charpy impact strength	ISO 179/1eA	KJ/m²	8
Tensile strength at break	ISO 527-2	MPa	42
Elongation at break	ISO 527-2	%	2
Tensile modulus	ISO 527-2	MPa	3100
Flexural modulus	ISO 178	MPa	2900
Rockwell hardness	ISO 2039-2		L 70
Electrical			
Dielectric strength		kV/mm	135
Surface resistivity	ISO IEC 93	Ohms	>10 E+14
Miscellaneous			
Density	ISO 1183	g/cm³	1.05
Moulding shrinkage		%	0.4-0.7
Water absorption	ISO 62	%	<0.1

General Information

- Standard properties: All tests carried out at 23°C unless otherwise stated. Mechanical properties are measured on injection moulded tests specimens.
- Bulk density: bulk density is approximately 0.6 g/cm3.
- Please refer to the Safety Data Sheet for further information.
- Please refer to the safety data sheet (SDS) for handling and storage information. It is advisable to convert the product within six months after delivery provided storage conditions are used as given in the SDS of our product. SDS may be obtained from the website: www.totalrefiningchemicals.com

TOTAL RESEARCH & TECHNOLOGY FELUY
Zone Industrielle C
B-7181 Feluy
Belgium

July 2013

Product Information

Mar 2017

Ultraform® H 2320 006 UNC Q600

Polyoxymethylene

BASF
We create chemistry

Product Description

Ultraform H 2320 006 UNC Q600 is a POM with high molecular weight grade for injection molding.

Applications

Typical applications include thick-walled articles.

PHYSICAL	ASTM Test Method	Property Value
Specific Gravity	D-792	1.40
Mold Shrinkage (1/8" bar, in/in)		0.02
Moisture, %	D-570	
(50% RH)		0.2
(Saturation)		0.8
MECHANICAL	**ASTM Test Method**	**Property Value**
Tensile Strength, Yield, MPa (psi)	D-638	
23C (73F)		64 (9,280)
Elongation, Yield, %	D-638	
23C (73F)		11
Flexural Modulus, MPa (psi)	D-790	
23C (73F)		2,450 (355,000)
IMPACT	**ASTM Test Method**	**Property Value**
Notched Izod Impact, J/M (ft-lbs/in)	D-256	
-40C (-40F)		69.4 (1.3)
23C (73F)		80.1 (1.5)
THERMAL	**ASTM Test Method**	**Property Value**
Melting Point, C(F)	D-3418	166 (330)
Heat Deflection @ 264 psi (1.8 MPa) C(F)	D-648	96 (204)
Heat Deflection @ 66 psi (.45 MPa) C(F)	D-648	154 (309)
Coef. of Linear Thermal Expansion, mm/mm C (in/in F)	E-831	0.6 X10-4
ELECTRICAL	**ASTM Test Method**	**Property Value**
Volume Resistivity (Ohm-m)	D-257	1E13
Surface Resistivity (Ohm)	D-257	1E13

Processing Guidelines

Material Handling

Max. Water content: 0.15%

Product is supplied in polyethylene bags and drying prior to molding is not required. However, after relatively long storage or when handling material from previously opened containers, preliminary drying is recommended in order to remove any moisture which has been absorbed. If drying is required, a dehumidifying or desiccant dryer operating at 80 - 110C (176 - 230F) is recommended. Drying time is dependent on moisture level, however 2-4 hours is generally sufficient. Further information concerning safe handling procedures can be obtained from the Safety Data Sheet. Alternatively, please contact your BASF representative.

Typical Profile

BASF Corporation
Engineering Plastics
1609 Biddle Avenue
Wyandotte, MI 48192

General Information: 800-BC-RESIN
Technical Assistance: 800-527-TECH (734-324-5150)
Web address: http://www.plasticsportal.com/usa

BASF
We create chemistry

® = registered trade mark of BASF SE

Ultramid® B40 LN

Product description

Ultramid® B40 LN is a polyamide 6 grade of high viscosity that is well suited for the production of blown and cast film. Clarity and thermoformability are enhanced by the incorporation of nucleating and slip agent.

Specification	**Test method**	**Unit**	**Value**
Relative Viscosity (RV) 1% [m/v] in 96% [m/m] sulfuric acid	According to ISO 307 (calculated by Huggins method)		3.89 - 4.17
Viscosity Number (VN) 0,5% [m/v] in 96% [m/m] sulfuric acid	According to ISO 307	ml/g	240 - 260
Moisture content	According to ISO 15512	% [m/m]	max. 0.06
Extractables	According to ISO 6427-chips not ground/16h	% [m/m]	max. 0.6
Lubricant	BASF method	(mg/kg)	250 - 550
Nucleating agent	BASF method	(mg/kg)	250 - 550
Film grade	BASF method		1 - 3

General properties	**Test method**	**Unit**	**Typical value**
Melting point	According to ISO 3146	°C	220
Density	According to ISO 1183	g/cm^3	1.12 - 1.15
Bulk density		kg/m^3	780
Pellet size		mm	2 - 2.5
Pellet shape			round
Water absorption, 23°C/50% rh		%	2.6
Water absorption, saturation in water 23°C		%	9.5

Data Sheet [English units]

TOPAS® 5013L-10

Injection molding grade for optical applications

Cyclic Olefin Copolymer (COC)

Property	Value	Unit	Test Standard
Physical Properties			
Density	**1020**	kg/m³	ISO 1183
Melt volume rate (MVR) (260°C, 2.16kg)	**48**	cm³/10min	ISO 1133
Melt flow rate (MFR) (260°C, 2.16kg)	**43**	g/10min	calculated
Water absorption (23°C-sat)	**0.01**	%	ISO 62
Mechanical Properties			
Tensile modulus (1mm/min)	**460**	kpsi	ISO 527-3
Tensile stress at break (5mm/min)	**6700**	psi	ISO 527-3
Tensile strain at break (5mm/min)	**1.7**	%	ISO 527-3
Charpy impact strength @ 23C	**6.2**	ft-lbs/in²	ISO 179/1eU
Charpy notched impact strength @ 23°C	**0.8**	ft-lbs/in²	ISO 179/1eA
Thermal Properties			
Glass transition temperature (10°C/min)	**273**	°F	ISO 11357-1,-2,-3
DTUL @ 0.45 MPa	**261**	°F	ISO 75-1, -2
Vicat softening temperature B50 (50°C/h 50N)	**271**	°F	ISO 306
Flammability @1.6mm nom. thickn.	**HB**	Class	UL94
Electrical Properties			
Relative permittivity at 1-10 kHz	**2.35**	-	IEC 60250
Volume resistivity	**<1E14**	ohm×m	IEC 60093
Comparative tracking index CTI	**>600**	-	IEC 60112
Optical Properties			
Deg. of light transmission	**91.4**	%	ISO 13468-2
Refractive index	**1.533**	-	ISO 489

TOPAS Advanced Polymers
Tel: +49 (0) 1805-1-86727 (Europe)
Tel: +1 (859) 746-6447 (North America)
email: info@topas-us.com
Internet: www.topas.com

Processing Conditions for Injection Molding

TOPAS® 5013L-10

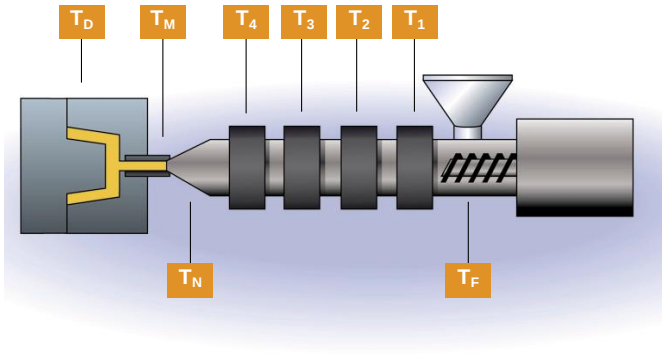

Processing temperatures:	T_F=< 100 °C < 212 °F T_1=230-260 °C 446-500 °F T_2=240-270 °C 464-518 °F T_3=250-280 °C 482-536 °F T_4=260-290 °C 500-554 °F T_N=240-300 °C 464-572 °F T_M=240-300 °C 464-572 °F
Mold-temperature:	T_D = 95 - 125 °C 203-257 °F
Max. residence time	< 15 min; short interruption to cycle: reduce T_x= 170°C (338°F) !
Injection pressure:	P_{Sp} = 500 - 1100 bar / 7- 16 kpsi (specific)
Hold on pressure:	P_N = 300 - 600 bar / 4- 9 kpsi (specific)
Back pressure:	P_{St} = 150 bar / 2200 psi max. (specific)
Screw speed:	n_s = 50 - 200 rpm
Injection speed:	moderate to fast (50 mm/sec - 150 mm/sec)
Nozzle type:	free - flow
Pre Drying:	100°C (212 °F) / 6hours

Note:

- Shrinkage is dependent on processing conditions and part design. Typical shrinkage values are 0,4 - 0,7%
- TOPAS Advanced Polymers recommends only external heated hot runner systems.
- For molded parts with especially high requirements to the surface quality we recommend to choose the highest possible mold temperature.

TOPAS
Thermoplastic Olefin Polymer of Amorphous Structure (COC)

TOPAS Advanced Polymers
Tel: +49 (0) 1805-1-86727 (Europe)
Tel: +1 (859) 746-6447 (North America)
email: info@topas.com
Internet: www.topas.com

Appendix B

Datasheets of coatings

PVD TECHNOLOGY & SPECIAL TOOLS

IMC

SCHEDA TECNICA RIVESTIMENTO

NOME	Diamond Like Carbon (DLC)
Formula	a-C:H
Tipologia	Multilayer Gradiente

TRIBOLOGIA	Valore	Norma di riferimento	Strumentazione
Spessore	2±0,5 µm	UNI 1071-2	Calotest
Adesione	55±4N	UNI 1071-3	Scratch Test
Durezza	2200±300HV	ISO 14577-1	Nanoindenter
Coefficiente di attrito	0,15±0,02	ASTM G99-04	Ball on disc
Rugosità	0,10±0,01µm	UNI 11255	Rugosimetro
Resistenza a Corrosione	1500 ore	ASTM B117-07a	Camera per SST

CHIMICA	Stechiometria (%)	Strumentazione
Cr	3	SEM-EDX
N	2	SEM-EDX
C	52	SEM-EDX
Si	10	SEM-EDX
H	33	

PRODUZIONE	Dato
Tecnologia	PaCVD
Evaporazione	Sputtering
Target	Cromo
Gas	Argon, Idrogeno , Azoto, Acetilene
Liquido	Silano

CERTIFICAZIONE	Approvazione
Procedura Interna ISO 9001	P-07.4
ISO TS 16949	Si
EN 1935	Si
ISO 10993	Si

PVD TECHNOLOGY & SPECIAL TOOLS

IMC

SCHEDA TECNICA RIVESTIMENTO

NOME	HDP Plastic
Formula	CrTiNbN
Tipologia	Bilayer

TRIBOLOGIA	Valore	Norma di riferimento	Strumentazione
Spessore	3±0,5 µm	UNI 1071-2	Calotest
Adesione	80±5N	UNI 1071-3	Scratch Test
Durezza	2973±263HV	ISO 14577-1	Nanoindenter
Coefficiente di attrito		ASTM G99-04	Ball on disc
Rugosità	0,17±0,05	UNI 11255	Rugosimetro
Resistenza a Corrosione	1500 ore	ASTM B117-07a	Camera per SST

CHIMICA	Stechiometria (%)	Strumentazione
Cr		
Ti		
Nb		
N		

PRODUZIONE	Dato
Tecnologia	PVD
Evaporazione	Arco
Target	Ti/Nb e Cr
Gas	Argon, Idrogeno , Azoto

CERTIFICAZIONE	Approvazione
Procedura Interna ISO 9001	P-07.4
ISO TS 16949	Si
EN 1935	No
ISO 10993	No

Appendix C

Datasheet of extractor rods used for cores

Z40/...

Auswerferstift, zylindrischer Kopf
Ejector pin, cylindrical head
Ejecteur à tête cylindrique

Mat.: WS (≈ 1.2516)
DIN 1530-1
gehärtet/hardened/trempé

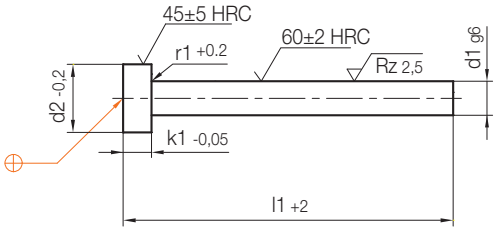

r1	k1	d2	d1	l1	Nr./No.
0,2	1,2	2,5	**0,8**	**40**	Z40/0,8x 40
				50	50
				63	63
				80	80
				100	100
				125	125
				160	160
			1	**40**	Z40/1 x 40
				50	50
				63	63
				80	80
				100	100
				125	125
				160	160
				200	200
			1,1	**40**	Z40/1,1x 40
				50	50
				63	63
				80	80
				100	100
				125	125
				160	160
				200	200
			1,2	**40**	Z40/1,2x 40
				50	50
				63	63
				80	80
				100	100
				125	125
				160	160
				200	200
	1,5	3	**1,3**	**40**	Z40/1,3x 40
				50	50
				63	63
				80	80

r1	k1	d2	d1	l1	Nr./No.
0,2	1,5	3	**1,3**	**100**	Z40/1,3x100
				125	125
				160	160
				200	200
			1,4	**40**	Z40/1,4x 40
				50	50
				63	63
				80	80
				100	100
				125	125
				160	160
				200	200
			1,5	**40**	Z40/1,5x 40
				50	50
				63	63
				80	80
				100	100
				125	125
				160	160
				200	200
				250	250
			1,6	**40**	Z40/1,6x 40
				63	63
				80	80
				100	100
				125	125
				160	160
				200	200
				250	250
			1,7	**40**	Z40/1,7x 40
				50	50
				63	63
				80	80
				100	100
				125	125

Appendix D

Datasheet of milling tool

2 FLUTE

STANDARD LENGTH BALL NOSE END MILLS

0.10mm - 6.00mm DIAMETER
Mirror Surface Finishes
Sub Micron Grain Carbide

Symbol Descriptions ➡ Page 7

STANDARD Length (Metric Sizes)

Dimensions (mm)				Uncoated		AlTiN Coating	
D +0.00mm −0.02mm	d^{h6}	ℓ	L	Part Number	Stock	Part Number	Stock
0.10	3	0.30	38	1625-0039.012	●	1625-0039L012	●
0.15	3	0.45	38	1625-0059.018	●	1625-0059L018	●
0.20	3	0.60	38	1625-0079.024	●	1625-0079L024	●
0.25	3	0.75	38	1625-0098.029	●	1625-0098L029	●
0.30	3	0.90	38	1625-0118.035	●	1625-0118L035	●
0.35	3	1.05	38	1625-0138.041	●	1625-0138L041	●
0.40	3	1.20	38	1625-0157.047	●	1625-0157L047	●
0.45	3	1.35	38	1625-0177.053	●	1625-0177L053	●
0.50	3	1.50	38	1625-0197.059	●	1625-0197L059	●
0.60	3	1.80	38	1625-0236.071	●	1625-0236L071	●
0.70	3	2.10	38	1625-0276.083	●	1625-0276L083	●
0.80	3	2.40	38	1625-0315.095	●	1625-0315L095	●
0.90	3	2.70	38	1625-0354.106	●	1625-0354L106	●
1.00	3	3.00	38	1625-0394.118	●	1625-0394L118	●
1.10	3	3.30	38	1625-0433.130	●	1625-0433L130	●
1.20	3	3.60	38	1625-0472.142	●	1625-0472L142	●
1.30	3	3.90	38	1625-0512.154	●	1625-0512L154	●
1.40	3	4.20	38	1625-0551.165	●	1625-0551L165	●
1.50	3	4.50	38	1625-0591.177	●	1625-0591L177	●
1.60	3	4.80	38	1625-0630.189	●	1625-0630L189	●
1.70	3	5.10	38	1625-0669.201	●	1625-0669L201	●
1.80	3	5.40	38	1625-0709.213	●	1625-0709L213	●
1.90	3	5.70	38	1625-0748.224	●	1625-0748L224	●
2.00	3	6.00	38	1625-0787.236	●	1625-0787L236	●
2.50	3	7.50	38	1625-0984.295	●	1625-0984L295	●
3.00	3	9.00	38	1625-1181.354	●	1625-1181L354	●
3.50	4	10.50	50	1625-1378.413	●	1625-1378L413	●
4.00	5	12.00	50	1625-1575.473	●	1625-1575L473	●
4.50	5	13.50	50	1625-1772.532	●	1625-1772L532	●
5.00	5	15.00	50	1625-1968.590	●	1625-1968L590	●
5.50	6	16.50	50	1625-2165.650	●	1625-2165L650	●
6.00	6	18.00	50	1625-2362.709	●	1625-2362L709	●

SERIES 1625 **WORKPIECE MATERIAL**

Coating	P Steel ~30HRC	P Steel 30~40HRC	H Hardened Steel ~55HRC	H Hardened Steel ~68HRC	M Stainless Steel	K Cast Iron	N Aluminum	N Graphite	N Copper Alloy	N CFRP	N Plastic	N Thermoset Plastic	N High Density Plastic	S Nickel / Cobalt	S Titanium Alloy
AlTiN	★	★	★	☆	☆	☆								☆	☆
Uncoated							☆	☆	★	☆	★	★			☆

★ : Priority ☆ : Applicable Materials

Symbol Descriptions ➡ Page 7

(U.S.) 1.888.848.8449
(International) 001.714.428.3636
Pricing & Availability at KyoceraPrecisionTools.com

U.S. Stock Standard : ●
NOT STOCKED - Call for Delivery : ■
Coming Soon : ▲

Bibliography

[1] Roger Artigas. "Imaging Confocal Microscopy". In: *Optical Measurement of Surface Tipography*. Ed. by Richard Leach. Berlin: Springer-Verlag, 2011.

[2] Usama M. Attia and Jeffrey R. Alcock. "Optimising process conditions for multiple quality criteria in micro-injection moulding". In: *The International Journal of Advanced Manufacturing Technology* 50.5 (2010), pp. 533–542.

[3] Usama M. Attia, Silvia Marson, and Jeffrey R. Alcock. "Micro-injection moulding of polymer microfluidic devices". In: *Microfluidics and Nanofluidics* 7.1 (2009), pp. 1–28.

[4] Omar M. Bataineh and Barney E.s Klamecki. "Prediction of local part-mould and ejection force in injection molding". In: *Journal of Manufacturing Science and Engineering* 127,3 (2005), pp. 598–604.

[5] Wittman Battenfeld GmbH. *MicroPower 5 – 15 t. Perfect business performance for nano and micro parts*. Technical documentation. 2010.

[6] Gerald Berger, Clemens Steffel Friesenbichler, and Gernot Pacher. "Prediction of friction in injection molding by wetting parameters". In: *6th International PMI Conference Proceedings* (2014), pp. 61–66.

[7] G.R. Berger, C. Steffel, and W. Friesenbichler. "A study on the role of wetting parameters in friction in injection moulding". In: *International Journal of Materials and Product Technology* 52.1-2 (2016), pp. 193–211.

[8] G.R. Berger, C. Steffel, and W. Friesenbichler. "On the Use of Interfacial Tension Parameter to Predict Reuction of Friction by Mold

Coatings in Injection Molding of Polyamide 6". In: *AIP Conference Proceedings* 1779 (2016).

[9] G.R. Berger et al. "Demolding Forces and Coefficients of Friction in Injection Molding. A new Practical Measurement Apparatus". In: Conference Proceedings of 67th Annual Technical Conference of the Society of Plastic Engineers. ANTEC, 2009, pp. 1699–1703.

[10] Michaela Anna Brandl. "Analysis of the demoulding friction of micro mould inserts fabricated by micro-EDM". Tesi di Laurea Magistrale. Università degli Studi di Padova, 2016.

[11] C. Burke and R. Malloy. *An Experimental Study of the Ejection Forces Encountered During Injection Molding*. ANTEC, pp. 1781–1787.

[12] Jean-Yves Charmeau et al. "Influence of mold surface coatings in injection molding. Application to the ejection stage". In: *International Journal of Material Forming* 1 (2008), pp. 699–702.

[13] Andrea Coloschi. "Analisi delle forze di estrazione nel microstampaggio ad iniezione al variare della finitura superficiale dello stampo dei parametri di processo". Tesi di Laurea Magistrale. Università degli Studi di Padova, 2016.

[14] M.S. Correira et al. "Modelling friction in the demoulding of injectio moulding". In: International Conference on Polymers and Moulds Innovations - PMI. University on Minho, Guimarães, Portugal. 2014.

[15] P.A. Dearnley. "Low friction surfaces for plastic injection moulding dies—an experimental case study". In: *Wear* 225-229 (1999), pp. 1109–1113.

[16] Kevin D. Delaney and Franck Lacan. "An Experimental Report of the Force Required to Demould Parts Replicated by Injection Moulding". In: Proceedings of the 4M/ICOMM2015 Conference. International Institution for Micromanufacturing. Milan, Italy, 2015.

[17] Kevin D. Delaney et al. "An investigation of the effect of surface carachteristics on adhesion beetween polymer melts and replication tools". In: Conference Proceedings of 70th Annual Technical Conference of the Society of Plastic Engineers. ANTEC, 2012, pp. 1847–1852.

[18] Kevin Delaney, David Kennedy, and Giuliano Bissacco. *Study of Friction Testing Methods Applicable to Demoulding Force Prediction for Micro Replicated Part*. Dublin Institute of Technology, 2010.

[19] J. Fleischer and I. Behrens. "Quality Assurance and Dimensional Measurement Technology". In: *Advanced Micro & Nanosystems. Volume 3. Microengineering of Metals and Ceramics. Part I. Design, Tooling and*

Injection Molding. Ed. by Detlef Löhe and Jürgen Haußelt. Weinheim: WILEY-VCH Verlag GmbH & Co., 2005.

[20] Marco Galzenati. "Analisi delle proprietà di bagnabilità dei rivestimenti superficiali per stampi effetto sul processo di stampaggio ad iniezione". Tesi di Laurea Magistrale. Università degli Studi di Padova, 2016.

[21] Alan B. Glanvill. *The Plastics Engineer's Data Book*. London: Machinery Publishing Co., Ltd., 1973.

[22] C.A. Griffiths et al. "Characterisation of demoulding parameters in micro-injection moulding". In: *Microsystem Technologies* 21.8 (2014), pp. 1677–1690.

[23] C.A. Griffiths et al. "Influence of Injection and Cavity Pressure on the Demoulding Force in Micro-Injection Moulding". In: *Journal of Manufacturing Science and Engineering* 136.3 (2014).

[24] C.A. Griffiths et al. "Investigation of surface treatment effects in micro-injection moulding". In: *The International Journal of Advanced Manufacturing Technology* 47 (2010), pp. 99–110.

[25] C.A. Griffiths et al. *Micro-Injection moulding: surface treatment effects on part demoulding*. Cardiff: Cardiff University, 2008.

[26] M. Heckele and W.K. Schomburg. "Review on micro molding of thermoplastic polymers". In: *Journal of Micromechanics and Microengineering* 14.3 (2004), R1–R13.

[27] V. Hegadekatte, N. Huber, and O. Kraft. "Development of a Simulation Tool for Wear in Microsystems". In: *Advanced Micro & Nanosystems. Volume 3. Microengineering of Metals and Ceramics. Part I. Design, Tooling and Injection Molding*. Ed. by Detlef Löhe and Jürgen Haußelt. Weinheim: WILEY-VCH Verlag GmbH & Co., 2005.

[28] K.M.B. Jansen, D.J. Van Dijk, and M.H. Husselman. "Effect of processing conditions on shrinkage in injection molding". In: *Polymer Engineering & Science* 38.5 (1998), pp. 838–846.

[29] Shen Kaizhi, Li-Min Chen, and Long Jiang. "Calculation of ejection force of hollow, thin walled, and injection moulded cones". In: *Plastic, rubber and composites* 28.7 (1999), pp. 341–345.

[30] Mary E. Kinsella. "Ejection Forces and Static Friction Coefficients for Rapid Tooled Injection Mold Inserts". PhD thesis. 2004.

[31] M.E. Kinsella et al. *Ejection forces and friction coefficients from injection molding experiments using rapid tooled inserts*. Technical report. DTIC Document. 2004.

[32] S. Kwak et al. "Layout and sizing of ejector pins for injection mould desian using the wavelet transform". In: *Proceedings of the Institution of Mechanical Engineers, Part B: Journal of Engineering Manufacture* 217.4 (2003), pp. 463–473.

[33] G. Lucchetta et al. "Effects of different mould coatings on polymer filling flow in thin-wall injection moulding". In: *CIRP Annals – Manufacturing Technology* 65.1 (2016), pp. 537–540.

[34] Davide Masato et al. "Impact of deep cores surface topography generated by micro milling on the demolding force in micro injection molding". In: *Journal of Materials Processing Technology* ().

[35] G. Menges and H. Bangert. "Measurement of Coefficients of Static Friction as a Means of Determining Opening and Demoulding Forces in Injection Moulds". In: *Kunststoffe* 71.9 (1981), pp. 552–557.

[36] W. Michaeli and R. Gärtner. "New Demolding Concepts for the Injection Molding of Microstructures". In: *Journal of polymer engineering* 26.2-4 (2006), pp. 161–178.

[37] Walter Michaeli and Bernhard Helbich. "Coupled FEA simulation of the demoulding procedure of injection moulded parts". In: (2008). Conference Proceedings of 66th Annual Technical Conference of the Society of Plastic Engineers, pp. 369–373.

[38] P. Mossadegh and D.C. Angstadt. "Micron and sub-micron feature replication of amorphous polymers at elevated mold temperature without externally applied pressure". In: *Journal of Micromechanics and Microengineering* 18.3 (2008).

[39] V.F. Neto et al. "(CVD) diamond-coated steel inserts for thermoplastic mould tools—Characterisation and preliminary performance evaluation". In: *Journal of Materials Processing Technology* 209.2 (2009), pp. 1085–1091.

[40] Pedro S. Nunes et al. "Cyclic olefin polymers: emerging materials for lab-on-a-chip applications". In: *Microfluidics and Nanofluidics* 9.2 (2010), pp. 145–161.

[41] Paolo Parenti et al. *Surface footprint in molds micromilling and impact on part demoldability in micro injection molding*.

[42] D. Pierick and R. Noller. "The effect of processing conditions on shrinkage". In: "In Search of Excellence". Conference Proceedings. Society of Plastic Engineers & Plastics Engineering. ANTEC, 1991, pp. 252–258.

[43] Miroslav Piska and Jitka Metelkova. "On the comparison of contact and non-contact evaluations of a machined surface". In: *MM Science Journal* 2 (2014), pp. 476–480.

[44] A.J. Pontes, A.M. Brito, and A.S. Pouzada. "Assessment of the ejection force in tabular injection moldings". In: *Injection Moulding Technology* 6.4 (2002).

[45] A.J. Pontes and A.S. Pouzada. "Ejection force in tubular injection moldings. Part I: Effect of processing conditions". In: *Polymer Engineering & Science* 44.5 (2004), pp. 891–897.

[46] A.J. Pontes et al. "Ejection force in tubular injection moldings. Part II: A prediction model". In: *Polymer Engineering & Science* 45.3 (2005), pp. 325–332.

[47] António José Vilela Pontes. "Shrinkage and ejection forces in injection moulded products". PhD thesis. Universidade do Minho, 2002.

[48] A.S. Pouzada, E.C. Ferreira, and A.J. Pontes. "Friction properties of moulding thermoplastics". In: *Polymer Testing* 25.8 (2006), pp. 1017–1023.

[49] Yi Qin. *Micro-Manufacturing Engineering and Technology*. 1st ed. Elsevier Inc., 2010.

[50] R. Ruprecht, G. Finnah, and V. Piotter. "Mocroinjection Molding – Principles and Challenges". In: *Advanced Micro & Nanosystems. Volume 3. Microengineering of Metals and Ceramics. Part I. Design, Tooling and Injection Molding*. Ed. by Detlef Löhe and Jürgen Haußelt. Weinheim: WILEY-VCH Verlag GmbH & Co., 2005.

[51] B. Saha et al. "A review on the importance of surface coating of micro/nano-mold in micro/nano-molding processes". In: *Journal of Micromechanics and Microengineering* 26.1 (2015).

[52] Tetsuo Sasaki et al. "An experimental study on ejection forces of injection molding". In: *Precision Engineering* 24.3 (2000), pp. 270–273.

[53] J. Schmidt and J. Kotschenreuther. "Micro End Milling of Hardened Steel". In: *Advanced Micro & Nanosystems. Volume 3. Microengineering of Metals and Ceramics. Part I. Design, Tooling and Injection Molding*. Ed. by Detlef Löhe and Jürgen Haußelt. Weinheim: WILEY-VCH Verlag GmbH & Co., 2005.

[54] J. Schneider, Zum Gahr K.-H., and J. Herz. "Tribological Characterization of Mold Inserts Materials for Microcomponents". In: *Advanced Micro & Nanosystems. Volume 3. Microengineering of Metals and Ceramics. Part I. Design, Tooling and Injection Molding*. Ed. by Detlef Löhe and Jürgen Haußelt. Weinheim: WILEY-VCH Verlag GmbH & Co., 2005.

[55] Steffen Gerhard Scholz. "Micro Injection Moulding: Process Monitoring and Optimisation". PhD thesis. Cardiff University, 2011.

[56] Marco Sorgato, Davide Masato, and Giovanni Lucchetta. "Effects of different mold surface coatings on the ejection force in micro ejection molding". In: Atti del XIII Convegno dell'Associazione Italiana di Tecnologia Meccanica. AITEM. Pisa, 11-13 settembre 2017.

[57] R. Surace et al. "The Micro Injection Moulding Process for Polymeric Components Manufacturing". In: *New Technologies – Trends, Innovations and Research*. Ed. by Constantin Volosencu. 2012.

[58] George M. Whitesides. "The origins and the future of microfluidics". In: *Nature* 442 (2006), pp. 368–373.

[59] M. Worgull et al. "Characterization of Friction during the Demolding of Microstructures Molded by Hot Embossing". In: Conference Proceedings. DTIP. Stresa, Italy, April 26–28: TIMA Editions, 2006.

[60] T.V. Zhiltsova, Oliveira M.S.A., and J.A. Ferreira. "Integral approach for production of thermoplastics microparts by injection moulding". In: *Journal of Materials Science* 48.1 (2013), pp. 81–94.

[61] G. Zitzenbacher et al. "Influence of tool surface on wall sliding of polymer melts". In: *International Journal of Materials and Product Technology* 52.1-2 (2016).